INFLUENCE OF WILDFIRE SOIL-BURN SEVERITY ON POST-FIRE DEBRIS FLOW OCCURRENCE

A Thesis

by

DEREK CHEUNG

Submitted to the Office of Graduate and Professional Studies of
Texas A&M University
in partial fulfillment of the requirements for the degree of

MASTER OF SCIENCE

Chair of Committee,	John R. Giardino
Committee Members,	HongBin Zhan
	Bradford Wilcox
Head of Department,	Ronald Kaiser

May 2021

Major Subject: Water Management and Hydrological Science

ABSTRACT

As climate continues to change under the weight of anthropogenic forcing, wildfires respond in kind. In fire-abundant southern California, wildfire incidents are increasing in frequency and magnitude causing widespread short- and long-term complications to human society while also altering natural ecosystems. Though current research anticipates changes to largescale fire regimes (the "new normal"), such as increases in future fire incidents and burn severities, predictive studies that analyze changes in ecosystem responses to changing fire regimes are still lacking. As a result, questions surrounding future trends in post-fire erosion patterns arise. Specifically, will an increase in wildfire soil-burn severity result in more post-fire debris flows? Answering this question is critical for increased human resiliency in light of climate change given the relative historical abundance of post-fire debris flows in the region, intensifying climate patterns, and continued acceleration of human development and densification of the Wildland Urban Interface (WUI). This research addressed this concern by utilizing a descriptive approach to analyze southern Californian post-fire debris flows from 2001 to 2018. It was found that if fire patterns continue to intensify, the number of post-fire debris flows in the region will also increase. This finding highlights the interconnectivity between natural erosive processes, wildfires, humans, and climate change.

DEDICATION

To my beautiful home state of California, my wonderful friends, and loving family.

"This one's for home."

ACKNOWLEDGEMENTS

I would like to thank my committee chair, Dr. John R. Giardino, and my committee members, Dr. HongBin Zhan, and Dr. Bradford Wilcox, for their guidance and support throughout the course of this research.

Thanks also go to my friends and colleagues and the department faculty and staff for making my time at Texas A&M University a great experience. Many thanks go to Ben Grunau and Jackie Rambo for their input, support, and extraordinary friendship, without which my time would not nearly be as enjoyable nor so full of wonderful memories. I am also extremely grateful for our pets Megan Grunau-Rambo, Biscuit Foo, and Wiggles Cheung for their emotional support.

I extend my thanks to my friends back home for their encouragement and unwavering friendship. I thank them for helping me feel at home when I am "alone" half-a-country away.

Finally, a million thanks to my loved ones. I thank my brother, mother, father, and my entire family for their encouragement, support, patience, sacrifice, and undying love. Without the assistance of my brother and father, my field surveys would not have been so memorable, nor would I have been able to share those spectacular montane views with those I love. Special thanks also, undoubtedly, go to my beautiful girlfriend, Siu Sahn Foo, for her patience, emotional support, compassion, and exceptional love. Her joyous, loving demeanor offered sanctuary in trying times, thus greatly improving the quality of my work. Completion of the overall project would have been impossible without these outstanding individuals.

CONTRIBUTORS AND FUNDING SOURCES

Contributors

This work was supervised by a thesis committee consisting of Dr. John R. Giardino (advisor), Dr. HongBin Zhan, and Dr. Bradford Wilcox of the Department of Water Management and Hydrological Science.

All work conducted for the thesis was completed by the student independently.

Funding Sources

Graduate study was supported by a scholarship from Texas A&M University, a department scholarship from the Water Management and Hydrological Science Department, and the Segal AmeriCorps Education Award.

No further funding was received for the completion of the research.

NOMENCLATURE

BAER	Burned Area Emergency Response Team
DEM	Digital Elevation Model
dNDVI	Differenced normalized difference vegetation index
ESRI	Environmental Systems Research Institute
NPS	National Park Service
IDW	Inverse Distance Weighted
m	meter
mm	millimeter
mm/h	millimeters per hour
km	kilometer
km^2	kilometers squared
NDVI	Normalized difference vegetation index
NEXRAD	Next Generation Weather Radar
NRCS	Natural Resources Conservation Service
SBS	Soil burn severity
STATSGO	The State Soil Geographic Database
SSURGO	Soil Survey Geographic Database
USDA	United States Department of Agriculture
USFS	United States Forest Service
USGS	United States Geological Survey
WUI	Wilderness Urban Interface

TABLE OF CONTENTS

Page

LIST OF FIGURES

FIGURE Page

LIST OF TABLES

1. INTRODUCTION

1.1 Background

Southern California is no stranger to wildfires, but a changing climate and recent events highlight the importance of understanding potentially new, deadly trends in post-fire ecosystem responses. Globally, surface temperatures have risen, on average, 1^{o} C from 1901 to 2016 and are projected to increase by another 2.2^{o} C within the conterminous United States between 2021 and 2050 (Peterson and Littell, 2014; Wuebbles et al., 2017). During the wet season, precipitation events are estimated to increase in intensity and frequency across the United States (Wuebbles et al., 2017), thus, increasing propagation of flammable vegetation in western states (Littell et al., 2009). Studies not only agree on an overall increase in burn severity (Potter, 2017; Sommerfeld et al., 2018) and annual area burned (Vose et al., 2012) as a result of these human-induced climate change effects, but also a rise in large forest fire incidents (Wuebbles et al., 2017; Yue et al., 2013). In short, increasingly fire-friendly conditions (i.e., increasing fuel densities, more droughts, higher temperatures) that increase the likelihood of hillslope soil erosion, and other mass movement events exist (Cleetus and Mulik, 2014; Emmett, 1970; Handwerger et al., 2019; Jon E Keeley, 2008; Neary et al., 2008; Sankey et al., 2017; Vose et al., 2012). Mass movement is particularly problematic for hilly regions that experience wildfires, because hillslope erosion after a burn is usually associated with the loss of a protective-surface canopy, altered forest floor, and development of a water-repellent layer (Neary et al., 2008), made more susceptible to failure after intense precipitation (Staley et al., 2016).

Direct anthropogenic influences such as land-use practices have also influenced fire regimes, which is defined as a sum of five factors: “fuel consumption patterns, intensity and

severity, fire frequency, patch size, and seasonality" (Keeley, 2008b, p. 1557). Timber harvesting, forest clearing, and fire exclusion by grazing have changed the density and structure of fuels in the United States (Vose et al., 2012). Within drier regions of the country, the increased number of trees and fuels have increased fire sizes and intensities (Keane et al., 2008; Vose et al., 2012). Human development in the WUI, an area where human development is grouped near or adjacent wildland vegetation (Mowery et al., 2019), can produce fuel management related problems, such as the build-up of fuel on the land surrounding communities that lack sufficient funds to address this issue (Mowery et al., 2019). Newly developed WUI areas then increase the susceptibility of and challenges associated with wildfires because of common human sources of ignition (Balch et al., 2017; Mowery et al., 2019). Between 1992 and 2012, humans were responsible for 84% of over 1.5 million government-recorded fire incidences in the United States (Balch et al., 2017). Balch and others (2017) also discovered that human-ignited wildfires tripled the length of the fire season and burned an area seven times larger than that resulting from natural causes (i.e., predominantly lightning). Compared to the early 21st century, the total area burned will likely double by mid-century (Vose et al., 2012).

Following western wildfires, hydrologic soil erosion is a common ecosystem response (Keeley, 2008). Consumption of the litter layer and destruction of the weak surface soil structure can render the ground unstable (Hubbert et al., 2005). Precipitation following a burn can then result in overland flow, which can cause rill erosion of the bare ground surface; these rills sometimes form into drainage-sized incisions depending on precipitation, local lithology, and slope (Moody and Martin, 2001). The formation of a hydrophobic (water repellant) layer caused by recondensation of organic material in the soil can cause surficial erosion with the addition of rainfall (Hubbert et al., 2005). This is largely the result of the inability for water to adequately

infiltrate into the soil, and lower saturated hydraulic conductivities associated with increasing burn severities (Moody et al., 2016). Debris flows, landslides, and other mass movement events that follow then transport weathering products, sometimes up to thousands of years' worth of slope material, in a single event (McCoy, 2015).

Sediment transferred to a stream channel can then be deposited or further transported downstream (Reid and Dunne, 2016), creating a myriad of river morphologies. The various physical environments created by debris directly benefit organisms by providing suitable habitat, such as gravel for spawning fish, which in turn can have wide-ranging ecosystem and societal benefits (Bellamy et al., 1992). Sediment transported downslope constitutes much of the substrate human infrastructure is built upon, especially agriculture for which it provides nutrients. Upon discharge into the ocean, sediment from mountain regions become a part of coastal environments, where beaches are supplied with sand and alluvial fans give rise to wetlands (Bray et al., 1995). Debris flows play an important role in the local geomorphic cycle and landscape evolution (McCoy, 2015). In southern California, debris flows are the dominant means of sediment transport for small watersheds (Scott, 1971). As a result, erosion may be perceived as a damaging natural process when solely considering human development (Fig. 1), but it is vital on the larger scales of sediment budgets and littoral cells.

Figure 1. (a) Dwelling damaged by a 2018 Montecito debris flow along Romero Creek in Montecito, CA. (b) Boulders transported by debris flows along western Transverse Ranges with a 2 m human for scale. These flows were generated by the Thomas Fire and an intense rain event. Photograph credit: Derek Cheung, 2018.

Debris flows are a type of ecosystem response that readily occurs within steep mountain ranges of southern California (Fig. 2). They are defined here as fast-moving flows of mud and rock (Highland et al., 1997) that are generated "…when masses of poorly sorted sediment, agitated and saturated with water, surge down slopes in response to gravitational attraction" (Iverson, 1997, p. 245). Debris flows that occur after a wildfire are known as post-fire debris flows and are a product of fire patterns and erosion. These flows are generally triggered by high-intensity rainfall events and are hypothesized to differ from debris flows in unburned areas because of dominating rapid runoff processes in burned areas versus longer-term infiltration based processes in unburned areas (Cannon et al., 2008). In general, debris flows differ greatly from water flows and hyperconcentrated flows (Costa, 1988). Water flows and floods are Newtonian fluids in which water and sediment are separated into two distinct phases and sediment concentrations do not exceed ~40% by weight (Costa, 1988). Hyperconcentrated

flows, like water flows, also separate solids and fluid into two separate components during deposition, but contain ~40 to 70% solids by weight (Beverage and Culbertson, 1964; Costa, 1988) and act as the midpoint along the flow type spectrum. Debris flows occupy the end of this spectrum consisting of ~70 to 90% solids by weight and, unlike water and hyperconcentrated flows, sediment is "irreversibly entrained" allowing for no separation of sediment and liquid components in flow deposits (Costa, 1988).

Figure 2. Debris flow warning sign within San Bernardino National Forest along Hurkey Creek, CA near Lake Hemet. Photograph credit: Derek Cheung, 2020.

Before discussing post-fire erosion, it is imperative to describe wildfires with consistent terminology (Keeley, 2008; Lentile et al., 2006; Parsons et al., 2010). Standard USDA terminology and definitions were utilized. Fire intensity is described as "the amount of energy or heat released per unit time or area during the consumption of organic matter" (Keeley, 2008a;

Parsons et al., 2010, p. 3). Fire severity is separated into two different terms: soil-burn severity and vegetation-burn severity. Vegetation-burn severity (VBS) is "…the effect of a fire on vegetative ecosystem properties…the degree of scorch, consumption, and mortality of vegetation and the projected or ultimate vegetative recovery" (Lentile et al., 2006; Parsons et al., 2010, p. 3). Soil-burn severity (SBS) is defined as "…the effect of a fire on ground surface characteristics, including char, depth, organic matter loss, altered color and structure, and reduced infiltration" (Lentile et al., 2006; Parsons et al., 2010, p. 3). This study will primarily refer to SBS as it is the critical factor for this erosion-focused investigation. The effects of a fire are subsequently defined as the physical, biological, and ecological impacts resulting from a fire on the environment (National Wildlife Coordinating Group, 2001; Parsons et al., 2010).

Previous studies speculate that burn-severity measurements are ineffective proxies for predicting changes in post-fire hydrologic ecosystem responses such as debris flows (Doerr et al., 2006; Keeley, 2008; Robichaud et al., 2000). Instead, it is hypothesized that factors responsible for debris flows are multifactorial (Keeley, 2008) and topography, lithology, fire regimes, rates of weathering, groundwater levels, and precipitation patterns all play equally important roles (Cannon et al., 2001; Cannon et al., 2008; Johnson et al., 1991; Robichaud et al., 2000). The hypotheses by Doerr et al. (2006), Keeley (2008), and Robichaud et al. (2000), however, were either proposed with differing ecosystems compared to the scope of this study, without defining the spatial scales to which these assumptions apply or were applied to entire U.S. Forest Service Regions. Robichaud et al. (2000) proposed this generalization for Region 5, which encompasses all of California, a state known for its incredible diversity in climate, hydrology, geology, topography, and fire patterns. Though the study acknowledged that post-fire debris flows are likely a sum of these factors, many studies currently emphasize precipitation

as the leading determinant of post-fire debris flow occurrence (i.e., Cannon et al., 2008; Kean et al., 2011; Staley et al., 2020), because of the natural ability of water to mobilize available sediment. This emphasis assumes that the major variables affecting post-fire debris flow occurrence are precipitation patterns. In a recent study, Staley et al. (2020) showed a dominant recurrence interval of less than two years for rainfall intensities associated with post-fire debris flows in the southwestern United States. This finding, in theory, rendered triggering precipitation intensities "constant" along with geology, soils, and topography when predicting debris flow generation because triggering precipitation intensities are likely to occur every year or every other year. As a result, the next most variable factor for post-fire debris flow generation would be fire regimes, which are actively changing (Keane et al., 2008; Vose et al., 2012). As a result, this study acknowledged rainfall as a triggering mechanism, but proposed changing fire regimes, particularly SBS, to be large deterministic factors warranting further investigation given a changing climate.

The USGS currently employs a precipitation-focused debris flow prediction model that accounts for three rainfall intensities and two soil-burn severity classes (Cannon et al., 2010; Staley et al., 2016). The severity considerations did not account for possible sediment contribution from low SBS areas, nor recent events (i.e., 2010 onwards) (Staley et al., 2016). Training data for the model contained observations from multiple southern Californian geomorphic provinces with similar but different geomorphic processes. For example, the Transverse and Peninsular Ranges both experience wildfires, post-fire erosion, Mediterranean climates, and fire-adapted vegetation, but possess different storm trajectories and slightly different average temperatures. This is especially true when comparing the Los Angeles microclimate to that of San Diego. The temporal range of the USGS dataset was before

California experienced a drastic change in fire patterns, particularly acreage burned (CALFIRE, 2018). Further, the model utilized the STATSGO database that provides antecedent, pre-fire soil properties at a coarse 1:250,000 spatial scale (Schwartz and Alexander, 1995). These limitations demonstrated the need for detailed, smaller-scale studies to elucidate the applicability of these claims and practices to localized regions by analyzing longer and more-recent timescales.

1.2 Problem Statement

From these understandings of fire regimes, projected climate patterns, erosive events, and human influences, many questions surround the effects of anthropogenic actions on debris flow occurrence. This study assumes that geology, soils, topography, and triggering rainfall intensities to remain constant. Triggering rainfall intensities were assumed constant because of the results of Staley et al. (2020) and the use of their debris flow observations within this study. The study answered the following: if wildfires follow their projected increase in soil-burn severity, will there be more post-fire debris flows?

Currently, it is unknown if worsening fire patterns will influence the occurrence of post-fire, runoff-generated debris flows. This knowledge gap carries many implications for hazard planning and mitigation and forest management for areas throughout southern California with similar hydrology, geology, geography, fire return intervals, vegetation, soil moisture conditions, climate, and human development.

1.3 Objectives

This investigation addressed the research question: if wildfires follow their projected increase in soil-burn severity, will there be more post-fire debris flows? This was achieved by conducting a descriptive study that quantifies the number of debris flows along with their respective SBS densities and precipitation event to determine if a statistical relationship exists between SBS, precipitation, and occurrence of debris flows. To accomplish this, the following objectives were met:

a. Debris flow and source area identification
b. Debris flow characterization
c. Data processing and analysis

These objectives were then combined with the problem question to form the following testable hypotheses:

H_0: There will not be a higher number of post-fire debris flows occurring in watersheds with higher soil-burn severity densities than lower soil-burn severity densities. In other words, there is a random distribution of flows in relation to soil-burn severity.

H_1: There will be a higher number of post-fire debris flows occurring in watersheds with higher soil-burn severity densities than lower soil-burn severity densities.

2. STUDY AREA DESCRIPTION

Southern California was chosen as the study site given the relative abundance of wildfires, post-fire debris flows, and availability of scientific data. More specifically, the study area contained the Transverse Ranges and the northern reaches of the Peninsular Ranges (Fig. 3). The Transverse Ranges are a unique set of Californian mountain ranges that trend predominantly east – west averaging ~50 km in width and stretching ~500 km in length from the San Bernardino Mountains in the east to the Santa Ynez Mountains to the west (Morton and Yerkes, 1987), whereas also acting as the northern border of the Greater Los Angeles Region. Within this 500 km stretch of peaks, the Los Padres, Angeles, and San Bernardino National Forests, as well as a multitude of State and National Parks occupy most of the acreage. Major transportation conduits in the area include U.S. Highway 101, and Interstates 5, 10, and 15, respectively.

The northern portions of the Peninsular Ranges were also selected for this regional analysis of southern California because of their shared similarities with the Transverse Ranges. The northernmost 50 km of two sub-mountain ranges from the larger Peninsular Ranges system included in this study are the San Jacinto and Santa Ana Mountains. These sub-ranges form a ~50 km wide valley ~25 km south of the Transverse Ranges. This valley houses the cities of Corona, Hemet, Perris, and Temecula. Like the Transverse Ranges, Interstates 5, 10, and 15 traverse their perimeters. Major Federal and State jurisdictional units include the Cleveland National Forest, San Jacinto Wilderness, and San Jacinto State Park. In total, the population enclosed by this portion of the Peninsular Ranges, the Transverse Ranges, and the Pacific Ocean exceeds 18 million people.

Figure 3. Portions of the Transverse and Peninsular Ranges included in this study are outlined in blue. The two disconnected polygons south of the Transverse Ranges are the Santa Ana (western polygon) and San Jacinto Mountains (eastern polygon). Source: Cheung, 2021.

2.1 Geology and Geomorphology

The Transverse Ranges possess some of the most unique natural features in California. Granitic rocks dominate the geology of the San Gabriel and San Bernardino mountain ranges, whereas marine and non-marine sedimentary rock units occupy the majority of the ranges west of the San Gabriel Mountains (Jennings, 1959; Jennings and Strand, 1969; Morton and Yerkes, 1987; Rogers, 1967). Similar to the rest of the State, faults (mostly reverse) dominate the region

including what is arguably the most well-known transform fault: the San Andreas Fault. The fault separates two of the largest structural units in the area, the San Gabriel Mountains and the San Bernardino Mountains (Morton and Yerkes, 1987). Elevations range from average mean sea level at the Pacific Ocean to ~3,506 m at San Gorgonio Mountain. The steepness of the Transverse Ranges can be attributed to rapid uplift of the mountain range resulting from north-south compressive deformation along the fault between the North American and Pacific Plates (Scott and Williams, 1935; Wentworth et al., 1971). Major hydrographic features that incise and shape the ranges include the Santa Ynez, Santa Clara, Los Angeles, San Gabriel, and Santa Ana rivers, as well as various creeks, streams, lakes, and reservoirs. Most of the creeks, streams, and rivers are immediately routed through detention/debris basins before exiting the mountain front through channelized reaches. As a result, little to no geomorphic change is observed within heavily urbanized areas after channelization.

The Peninsular Ranges to the south share many similar characteristics with their sister ranges previously mentioned. The analyzed section of the Santa Ana Mountains is dominated by Mesozoic sedimentary rocks with some Mesozoic granitic rocks dispersed within. The San Jacinto Mountains are occupied by predominantly Mesozoic granitic rocks and Pre-Cretaceous metamorphic rocks (Rogers, 1965). Arguably, the more regularly observed north-south orientation of the ranges is the most noticeable difference between the Peninsular ranges and the Transverse Ranges given differing tectonic activity (Jahns, 1954). Numerous faults crisscross the Peninsular Ranges, two of the largest are the Elsinore and San Jacinto strike-slip faults that are both located within the Pacific Plate (Rogers, 1965). Following this, local steepness mimics that of the Transverse Ranges where elevations reach about 3,302 m at San Jacinto Peak. Parts of these mountains also comprise the Santa Ana River watershed and contribute water to major

lakes in the area such as Lake Mathews, Lake Elsinore, Perris Reservoir, and Diamond Valley Lake. Major surficial fluvial conduits in the area are also subjected to debris/detention basins and channelization because of the high degree of human development.

2.2 Climate

The local climate can be attributed in large part to the Pacific Ocean and the surrounding land mass. It is popularly described as "Mediterranean" with cool, wet winters and warm, dry summers (Scott and Williams, 1935). Droughts commonly accompany La Niña events (Woodhouse et al., 2020), whereas El Niño Southern Oscillations provide much of the local winter precipitation (Jong et al., 2016); both of which, are meteorological products of the interaction between the Pacific Ocean and of Earth atmosphere. Storms moving inland are also subject to orographic effects. Each year, Santa Ana winds, a foehn-type easterly or northeasterly, blow in from the deserts east of the ranges towards the Pacific Ocean bringing dry weather. As a result, diverse environments form and average annual precipitation in the area ranges from 381 mm per year in low lying areas to over 1,000 mm in higher elevations (NWS, 1995). This allows mountain vegetation to span a spectrum ranging from chaparral and oak woodlands in dryer areas to conifer forests in wetter alpine elevations (Minnich, 2007).

3. METHODS

3.1 Debris Flow and Source Area Identification

Before any analysis was undertaken, post-fire debris flows and their source areas were identified, and their locations documented. This step is critical in identifying the drainages to be analyzed in this study. The semi-stochastic nature of where and when post-fire debris flows occur has historically limited the availability of direct measurements by scientists to mostly post-event observational clues (i.e., Iverson, 1997; Kean et al., 2019). As a result, various post-fire debris flow studies agree upon similar lines of geomorphic evidence when attempting to confirm whether a debris flow occurred within a given drainage. To identify and verify the occurrence of post-fire debris flows, a dual verification method was developed similar to that employed by Lukashov et al. (2019).

The dual verification method involved remote sensing products that were assessed, and field verified for accuracy. PlanetScope 4-band aerial imagery scenes provided by Planet Team (2017) at 3 m spatial resolution (planet.com) were interpreted for observational clues (i.e., channel scour) to identify where debris flows occurred, and their source areas. Scenes were selected over fire footprints from the first cloudless day following a major storm that immediately preceded debris flows and the first cloudless image before fire ignition. These scenes were processed in Google Earth Engine® to produce Normalized Difference Vegetation Index (NDVI) (Fig. 4a. and Fig. 4b.) and differenced Normalized Difference Vegetation Index (dNDVI) (Fig. 4c.) products. NDVI products were used to produce dNDVI images that would identify drastic decreases in vegetation cover within stream channels; these clues were interpreted as possible evidence of channel scour and intense erosion. dNDVI products were

mainly used as supplementary material for debris flow identification. Field surveys affirmed or disproved observations from the remotely sensed products. Field clues typically included marginal levees, gullies, rills, channel scour, mud drapes, boulder deposits, matrix deposits, and points of debris impact (i.e., Iverson, 1997; Johnson et al., 2012; J W Kean et al., 2019; Jason W. Kean et al., 2011; Lukashov et al., 2019). Of these, marginal levees were considered a depositional trait unique to debris flows (i.e., Iverson, 1997; Lukashov et al., 2019) where the sediment-rich matrix entrains and diverts coarse material to the flow front where it then deposits along flow margins because of decreased velocity (Costa, 1988; Johnson et al., 2012). The other forms of geomorphic evidence may characterize other types of erosive events, such as hyperconcentrated flows, but when combined with observed marginal levees (Fig. 5), a debris flow likely occurred. Physical outlet locations, confirmation of source areas, number of flows per fire, and total number of debris flows would be acquired from this process. Fires investigated for flows were also constrained to 2001 onwards because that was when soil-burn severity maps were first made publicly available.

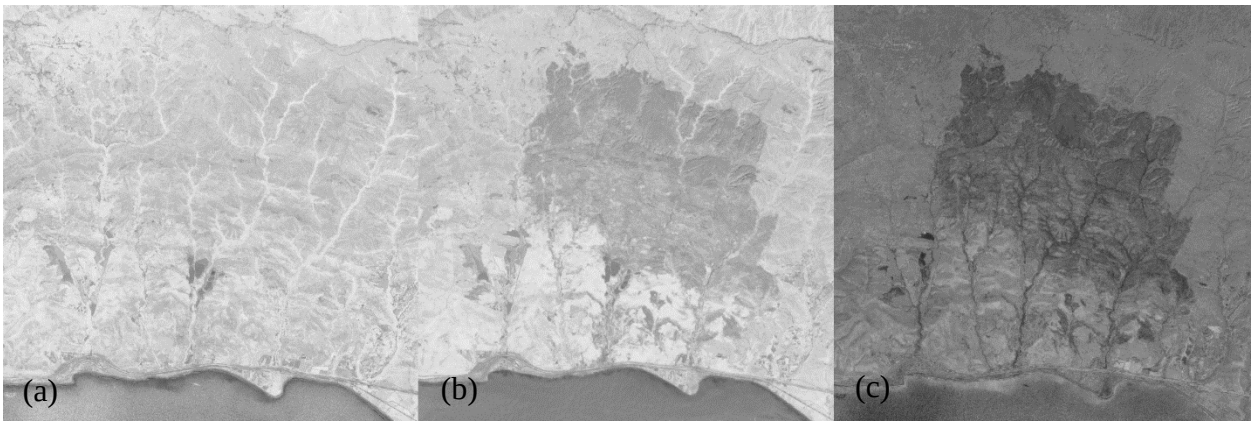

Figure 4. (a) Pre-fire NDVI product over the 2016 Sherpa fire in Santa Barbara, CA. (b) Post-debris flow and post-burn NDVI product. The burned area is portrayed darker (lower in vegetation) than surrounding areas. (c) dNDVI product where (a) was subtracted from (b) to generate negative NDVI values that indicate a heavy loss in vegetation. Note that large numbers of negative (black) values in (c) are focused within stream channels, thus suggesting intense scouring. Image source: Planet Team.

Figure 5. Example of a debris flow marginal levee with a 2m human as scale. This feature was observed immediately downstream of Horsethief Canyon, which was burned by the 2018 Holy Fire. Photograph credit: Derek Cheung, 2020.

Post-fire debris flows included in this study, but were not subject to this identification process were those recorded by Staley et al. (2016) (USGS), Tang et al. (2019), and Lukashov et al. (2019) (California Geological Survey). These debris flows were not identified using the methods previously mentioned because this study requires historical observations and those collected in these datasets provide the necessary temporal coverage. These documented observations were included given their rigorous documentation and or utilization of similar approaches adopted by this study.

3.2 Debris Flow Characterization

After debris flows have been confirmed and documented, their drainages were then individually characterized for spatial analysis. Watershed areas, contributing burn areas, SBS densities, precipitation peak 15-minute intensity estimates, major soil units, and slope distributions were all included for each debris flow observation. Publicly available data was gathered and processed in ESRI ArcMAP® version 10.5.

3.2.1 Watershed Delineation

Watershed boundaries are required to derive the drainage area for SBS density estimates, as well as for clipping relevant geospatial data. The furthest downstream in a channel where post-fire debris flow evidence was observed before it exited the mountain front determined the outlet point of the delineated watershed. In other words, all watersheds in this study will be contained within their respective mountain ranges to avoid lowland areas in the source area delineation process. The reasoning for this is that debris flows are generated in mountainous areas with steep reliefs (Costa, 1988; Iverson, 1997). Watersheds will then be generated from these outlet points utilizing 10m DEMs from the NRCS Geospatial Data Gateway (datagateway.nrcs.usda.gov). Ten m DEMs were chosen to better delineate small watersheds. The DEMs were also used to generate topographic products. The areas were calculated in square meters.

3.2.2 Wildfire Area and Soil Burn Severity

A major facet of this investigation is connecting a watershed with its pyric characteristics, specifically SBS densities and fire perimeters. Low SBS is characterized by recognizable, partially unconsumed surface organics with no structural change to soil aggregates and moderate SBS exhibits noticeably damaged soil aggregates and surface char, whereas high SBS is when nearly all pre-fire ground cover and surface organics are consumed with bare soil exposed to the elements and sediment erodibility is significantly higher (Parsons et al., 2010). Cartographic products of burned perimeters and SBS are generated by the USGS Center for Earth Resources Observation and Science, United States Forest Service (USFS) Geospatial Technology and Applications Center (GTAC), and USFS BAER teams.

Fire footprints and SBS distributions were retrieved from the Monitoring Trends in Burn Severity (mtbs.gov) website and the United States Department of Agriculture (USDA) Forest Service Remote Sensing Applications Center (fsapps.nwcg.gov) websites respectively for each fire studied. Quantitative descriptions of these products were generated for each watershed: fire-areal coverage, SBS density, SBS areal estimates, and dominant SBS classifications. A SBS classification was designated as "dominant" if it occupied at least 50% of the burned area within a debris flow watershed. Fire-areal coverage, in square meters, is defined as the amount of burned area within a debris flow watershed. SBS density estimates for drainages are defined as:

$$SBS_{density} = \frac{SBS_{unburned,low,moderate,high}}{A} \quad (1)$$

where, $SBS_{density}$ is the SBS density (unitless); $SBS_{unburned,low,moderate,high}$ is the area burned at predominantly unburned, low, moderate, or high SBS; and A is the burnt area contained within the delineated watershed. SBS data availability also constrained the study to 2001 onwards.

3.2.3 Precipitation Event

Precipitation events that immediately preceded the flows were documented over the drainage basins. This phase of characterization was included because water, specifically intense precipitation in the form of rain, is assumed as the triggering mechanism for a debris flow (Cannon et al., 2008) given its innate ability to mobilize sediment and debris. The results were also compared to the findings of Staley et al. (2020). Average rainfall intensity estimates over each watershed were generated with National Oceanic and Atmospheric Administration (NOAA) Next Generation Weather Radar (NEXRAD) and local-agency tipping bucket gauge stations. Tipping-bucket stations closest or entirely contained within the source areas were given the greatest weight when the IDW method was used to calculate peak 15-minute intensities in ArcMap®. The product was a peak 15-minute rainfall intensity estimate associated with each flow in millimeters per hour, as well as a general date and time estimate. These temporal characteristics were also used to calculate the time between burn and debris flow event.

3.2.4 Soils and Topography

Soil and topographic distributions were finally extracted for each drainage. These were both acquired from the USDA NRCS Geospatial Data Gateway. Areal coverage of prominent geological units was determined in ArcMap® to aid in describing soil material composition in square meters. A slope map will be generated using the 10m DEM mentioned in section 5.2.1 for every drainage basin that experienced a debris flow to characterize the steepness of the local

topography. Dominant slope intervals were then derived from the slope map to quantify the steepness of the terrain.

3.3 Data Processing and Analysis

All the data gathered was then distilled into meaningful, quantitative products. The number of post-fire debris flows associated with a SBS density of at least 0.5 were categorized and plotted. This step will better facilitate the visualization and achievement of the overall goal of the study: the number of flows associated with each dominant SBS classification. The number of post-fire debris flows were also compared with the other data collected in the study such as precipitation values and geologic distributions to help create a qualitative understanding of post-fire debris flows in the region. Statistical analyses such as Tukey's Test for differing means, ANOVA tables, Pearson correlation coefficients, R-squared value, and box and whisker plots accompanied the results. From these findings, a hypothesis was generated about the future frequency of occurrence of post-fire debris flow events in southern California.

4. RESULTS

The final dataset of post-fire debris flows compiled for this analysis consisted of 314 debris flows from twelve fires in southern California (Fig. 6). The dataset averaged 26.2 debris flows per fire with the Thomas, Station, and Grand Prix-Old fires containing the most (n=100, 95, and 60, respectively) (Fig. 7). The Grand Prix-Old fire was considered as a single fire event because it was a complex fire. Watersheds in the analysis were found to mostly drain towards southerly (southwest, south, southeast) directions towards the Pacific Ocean (Fig. 8). Over 50% of all flows drained in the south or southwesterly directions. Most (~55%) debris flow watersheds were found to possess slopes between 35 and 40 degrees (Fig. 9). These were followed by ~21% of debris flow watersheds sourced from 30 to 35-degree slopes. Debris flow watershed areas ranged from 0.03 to 32.31 km^2 and averaged around 2 km^2 per debris flow (Table 1). These areas also included non-burned areas. Statistics of burned areas within debris flow watersheds are discussed in section 6.1.

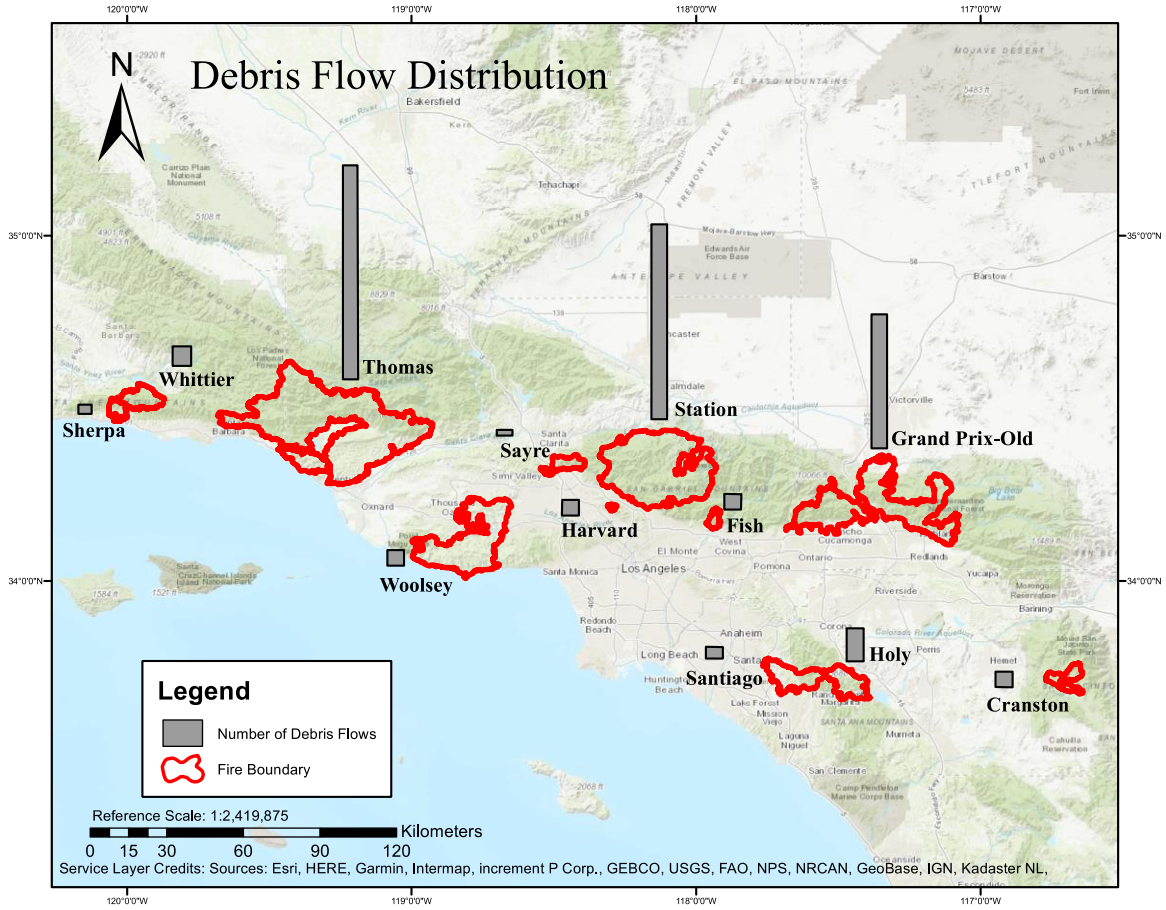

Figure 6. Distribution of debris flow dataset used in this study. The bars represent the number of debris flows observed for each fire where longer bars equal more debris flows. Source: Cheung, 2021.

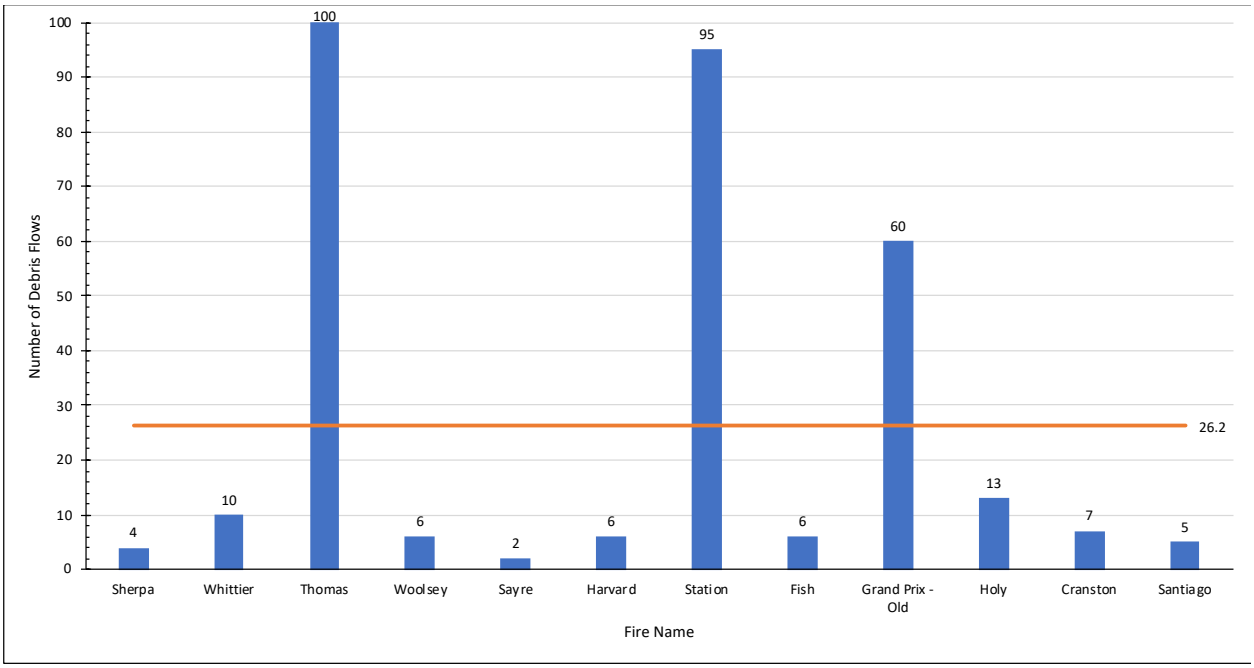

Figure 7. Debris flows observed for each fire. The average is presented as a solid line.

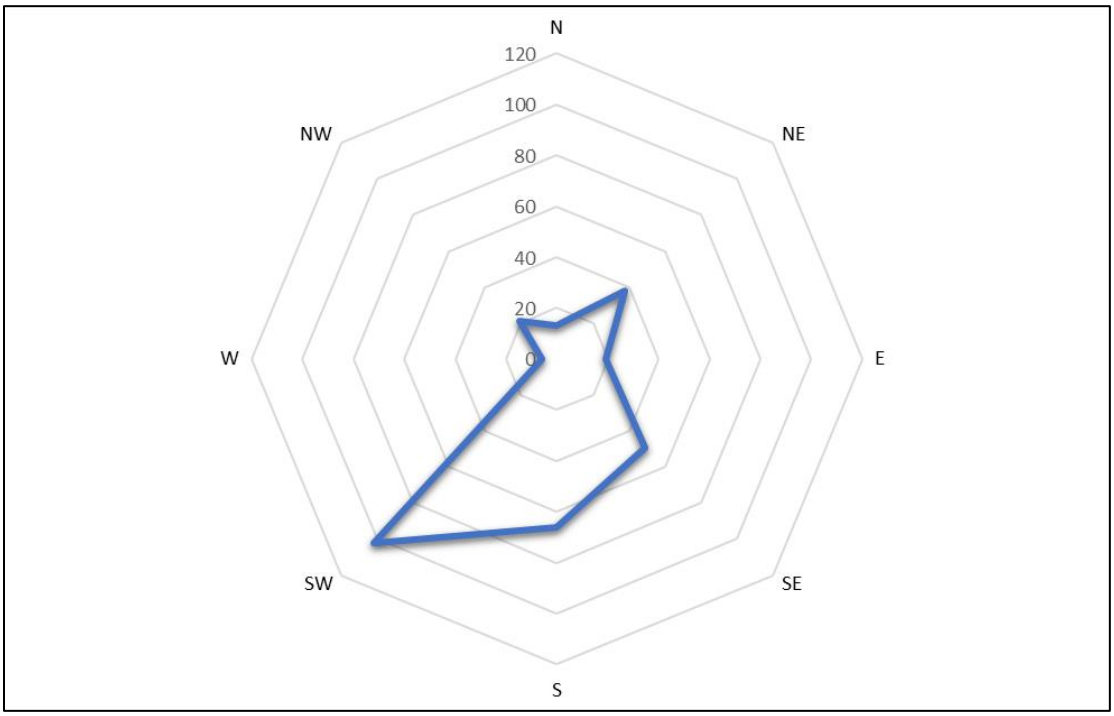

Figure 8. Cardinal direction debris flow watersheds are draining towards. A majority of watersheds seem to face towards the Pacific Ocean and Los Angeles Basin.

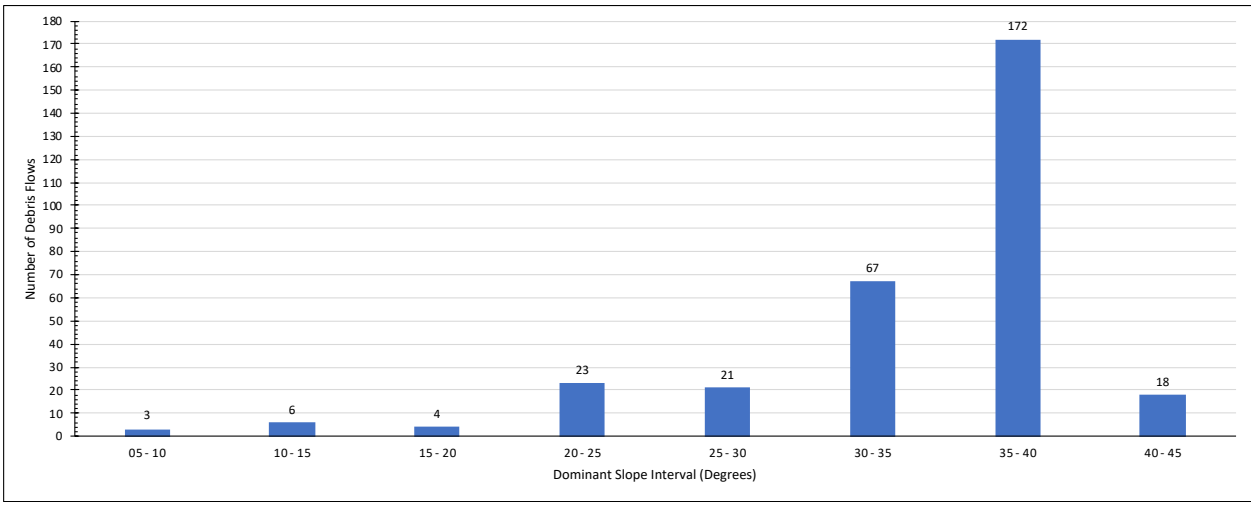

Figure 9. Dominant slope distribution of debris flows. Each interval represents 4.99 degrees of slope. For example, and interval of 10-15 equates to 10 to 14.99 degrees.

Table 1. Debris flow watershed area (km^2)

Mean	2.00
Median	0.62
Range	32.28
Minimum	0.03
Maximum	32.31
Sum	627.46

4.1 Debris Flows and Soil Burn Severity

When compared to SBS, a large majority of debris flows were associated with a single burn severity class (Fig. 10). Total area burned within each debris flow watershed was calculated to perform the density operation (Table 2). Over 84% (n=264) of debris flows in the dataset originated from moderate SBS source areas. These flows all possessed equal-to or greater-than 0.50 (50%) SBS densities for their watersheds. Watersheds predominantly burned at a low SBS accounted for 7.32% (n=23) of debris flows followed by unburned (2.23%) and

high (0.32%) SBS classifications. Subsequent analysis suggests that the number of debris flows could be inversely correlated with SBS density since unburned, low, and high SBS densities were given negative Pearson correlation coefficients (Table 3). Moderate SBS density was the only exception with a positive coefficient of ~0.834. In general, most SBS density intervals regardless of SBS classification were associated with less than 60 debris flows (Fig. 11).

Table 2. Burned area of debris flow watersheds (km^2)

Mean	1.81
Median	0.60
Range	24.55
Minimum	0.03
Maximum	24.58
Sum	568.31

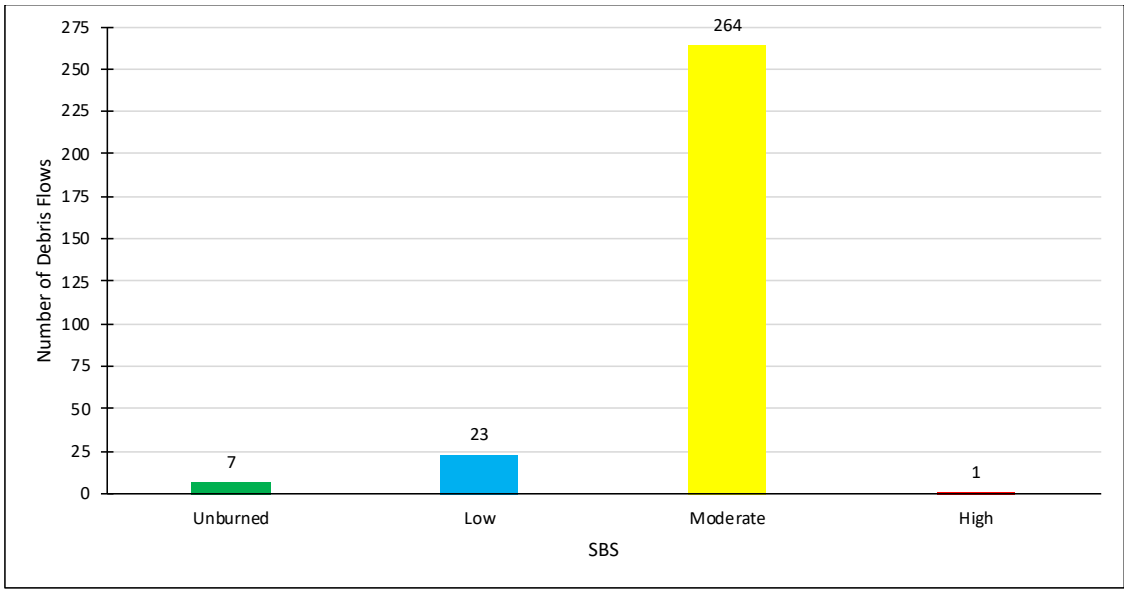

Figure 10. Debris flow distribution in relation to dominant SBS classification within a debris flow watershed. Dominant SBS conditions required the burnt area within a debris flow watershed to equal or exceed 50% of the total debris-contributing area. Numbers of observations are labeled above each SBS classification.

Table 3. Pearson correlation coefficients between SBS interval and number of debris flows

	Unburned Interval	*Number of Debris Flows*
Unburned Interval	1	
Number of Debris Flows	-0.44	1
	Low Interval	*Number of Debris Flow*
Low Interval	1	
Number of Debris Flow	-0.79	1
	Moderate Interval	*Number of Debris Flows*
Moderate Interval	1	
Number of Debris Flows	0.83	1
	High Interval	*Number of Debris Flows*
High Interval	1	
Number of Debris Flows	-0.47	1

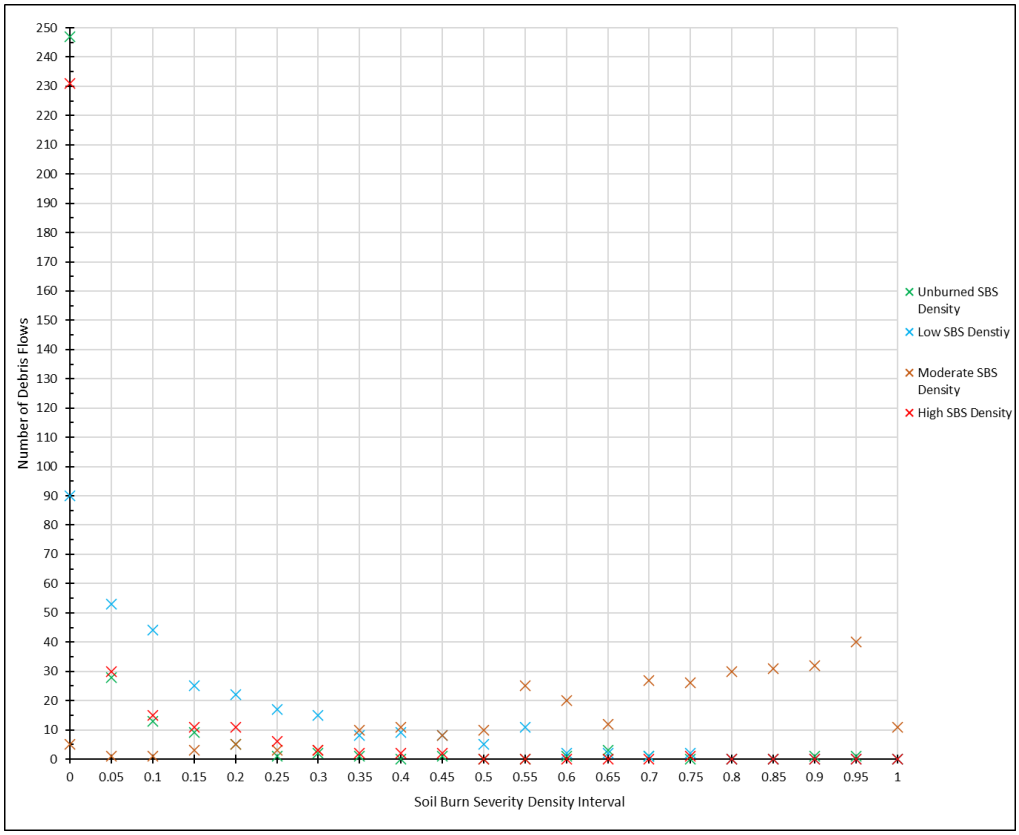

Figure 11. Distribution of debris flows associated with each SBS density interval. Every major unit represents the bottom of a 0.049 density interval. For example, an interval value of 0.1 represents density values from 0.1 to 0.149.

The distribution of SBS densities were also found to be, generally, statistically significant. Most (~75%) debris flows possessed a moderate SBS density greater than ~0.59 and 50% of debris flows had a moderate SBS density between ~0.59 and ~0.91 over their burnt areas (Fig. 12). This dominant SBS classification was followed by the low SBS density distribution. Tables of basic statistics (Table 4) and a single factor ANOVA analysis (Table 5) were generated to help assess any differences in average SBS density between SBS classifications. A low P-value combined with a F-statistic much larger than the F-critical value, suggested some differences between average SBS densities. A Tukey's HSD analysis with an alpha of 0.05

further analyzed this observation for specific differences between SBS classification means (Table 6). The test determined that except for the comparison between unburned and high SBS densities, all other comparisons between means were statistically different from one another.

Table 4. SBS density summary statistics

Groups	*Count*	*Sum*	*Average*	*Variance*
Unburned (1)	314	16.15	0.05	0.02
Low (2)	314	54.50	0.17	0.03
Moderate (3)	314	226.77	0.72	0.05
High (4)	314	16.27	0.05	0.01

Table 5. ANOVA single-factor analysis with alpha of 0.05 for SBS density

Source of Variation	*SS*	*df*	*MS*	*F*	*P-value*	*F crit*
Between Groups	96.56	3	32.19	1212.51	0	2.61
Within Groups	33.24	1252	0.03			
Total	129.80	1255				

Table 6. Tukey's HSD analysis for SBS density

SBS Group Comparisons	*Difference*	*n Group 1*	*n Group 2*	*Std Error*	*Q*	*Qcrit*	*Different Means?*
1 vs 2	0.12	314	314	0.01	13.28	3.69	Yes
1 vs 3	0.67	314	314	0.01	72.95	3.69	Yes
1 vs 4	0.00	314	314	0.01	0.04	3.69	No
2 vs 3	0.55	314	314	0.01	59.67	3.69	Yes
2 vs 4	0.12	314	314	0.01	13.24	3.69	Yes
3 vs 4	0.67	314	314	0.01	72.91	3.69	Yes

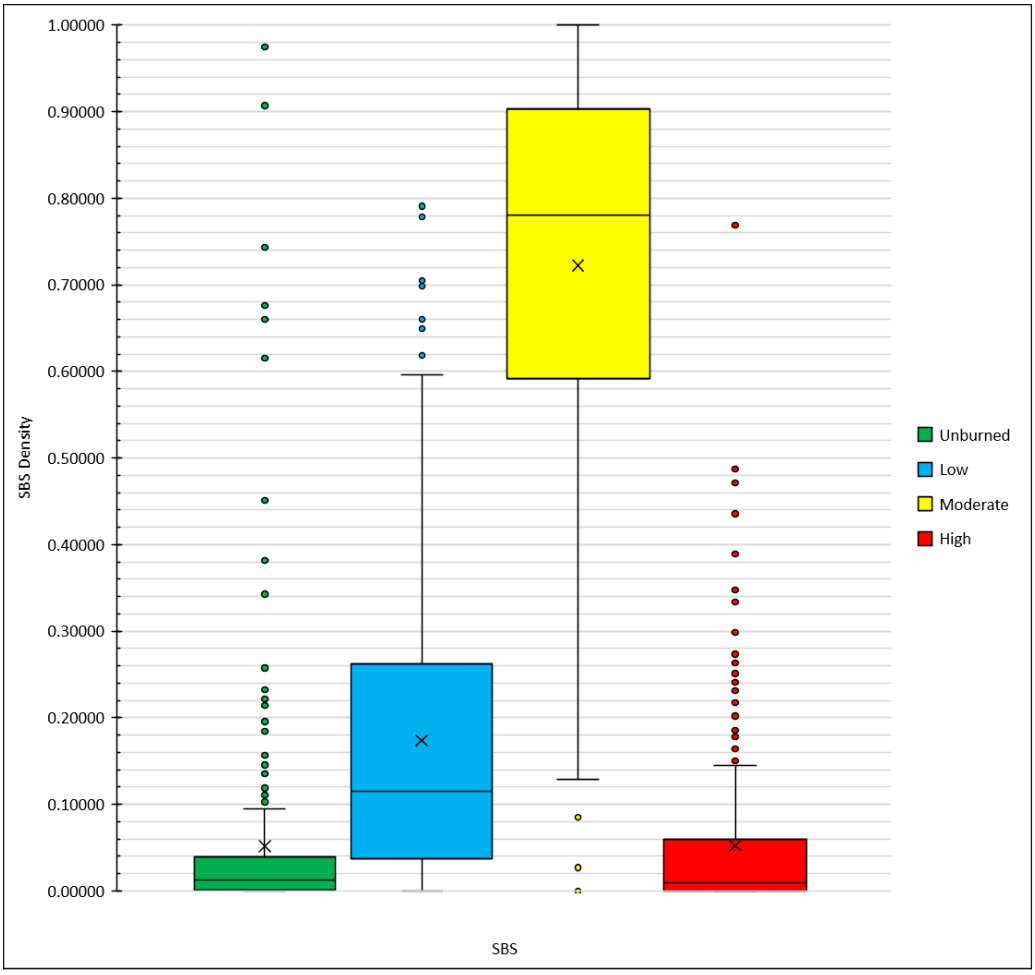

Figure 12. Box and whisker distribution of debris flow SBS densities grouped by SBS classification. The small crosses represent the means and individual points identify outliers.

Compared to the distribution of SBS densities, statistics of SBS areas and their respective number of debris flows produced more mixed results. Roughly ~50% of all moderate SBS areas range between ~0.16 and ~1.39 km^2, while unburned, low, and high SBS areas fall well below 0.25 km^2 (Fig. 13). Pearson correlation coefficient values all suggest an inverse correlation between the area burned under a SBS class and the number of debris flows (Table 7). The distribution of these values was also analyzed with a general statistics (Table 8) table and an ANOVA table (Table 9). Since the P-value was much smaller than 0.05 and the F-statistic was

also much larger than the F-critical value, the null hypothesis of equal means between SBS areas is rejected. A Tukey's HSD was conducted to analyze the specific differences in means (Table 10). The analysis suggests more related means between SBS areas than SBS densities. Unburned, low, and high SBS values are more related to one another, while the moderate SBS area mean is significantly different from the rest.

Table 7. Pearson correlation coefficients between SBS area and number of debris flows

	Unburned SBS Area	*Number of Debris Flows*
Unburned SBS Area	1	
Number of Debris Flows	-0.21	1
	Low SBS Area	*Number of Debris Flows*
Low SBS Area	1	
Number of Debris Flows	-0.37	1
	Moderate SBS Area	*Number of Debris Flows*
Moderate SBS Area	1	
Number of Debris Flows	-0.36	1
	High SBS Area	*Number of Debris Flows*
High SBS Area	1	
Number of Debris Flows	-0.18	1

Table 8. SBS area summary statistics

Groups	*Count*	*Sum*	*Average*	*Variance*
Unburned (1)	314	27.21	0.09	0.10
Low (2)	314	70.61	0.22	0.17
Moderate (3)	314	426.00	1.36	5.60
High (4)	314	44.08	0.14	0.21

Table 9. ANOVA single-factor analysis with alpha of 0.05 for SBS area

Source of Variation	*SS*	*df*	*MS*	*F*	*P-value*	*F crit*
Between Groups	345.60	3	115.20	75.82	4.61E-45	2.61
Within Groups	1902.38	1252	1.52			
Total	2247.98	1255				

Table 10. Tukey's HSD analysis for SBS area

SBS Group Comparisons	*Difference*	*n Group 1*	*n Group 2*	*Std Error*	*Q*	*Qcrit*	*Different Means?*
1 vs 2	0.14	314	314	0.07	1.99	3.69	No
1 vs 3	1.27	314	314	0.07	18.26	3.69	Yes
1 vs 4	0.05	314	314	0.07	0.77	3.69	No
2 vs 3	1.13	314	314	0.07	16.27	3.69	Yes
2 vs 4	0.08	314	314	0.07	1.21	3.69	No
3 vs 4	1.22	314	314	0.07	17.48	3.69	Yes

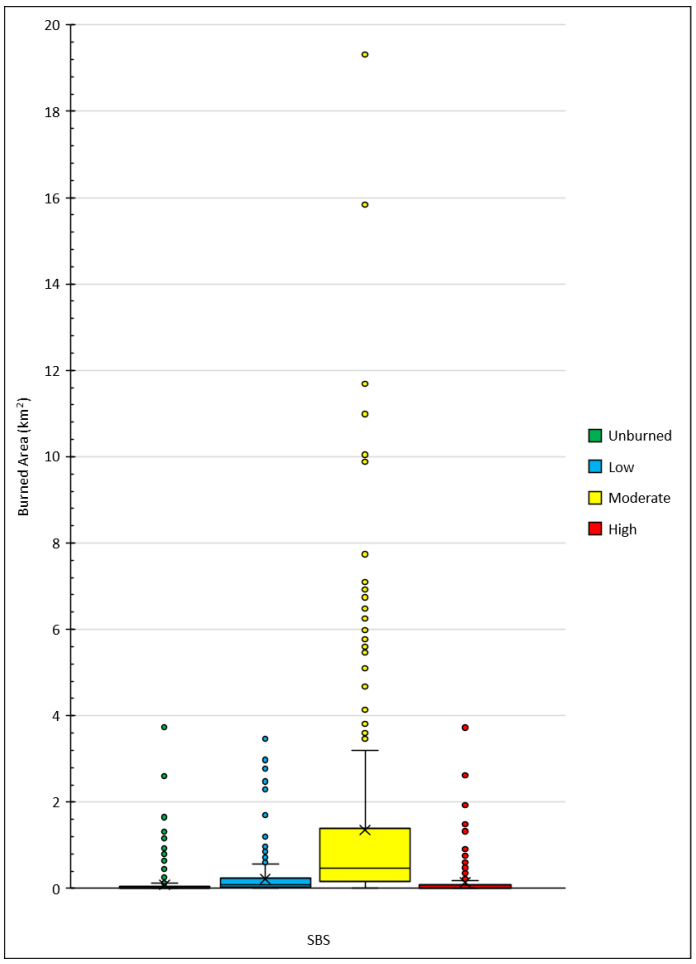

Figure 13. Box and whisker plot of SBS areal coverage within debris flow watersheds. Outliers are represented as points while means are represented by crosses.

4.2 Soil Burn Severity and Precipitation

A distribution of average, peak 15-minute rainfall intensities categorized by SBS showed moderate SBS exhibiting a higher average intensity (37.12 mm/hr) (Fig. 14). These results suggest debris flows originating from watersheds of predominantly (≥50% of burned area) moderate SBS are associated with higher rainfall intensities. The graph also shows less-intense rainfall causing debris flows in watersheds burned at high SBS when compared to unburned,

low, and moderate SBS classifications. The average peak 15-minute intensity over all SBS classifications was determined to be 28.64 mm/hr.

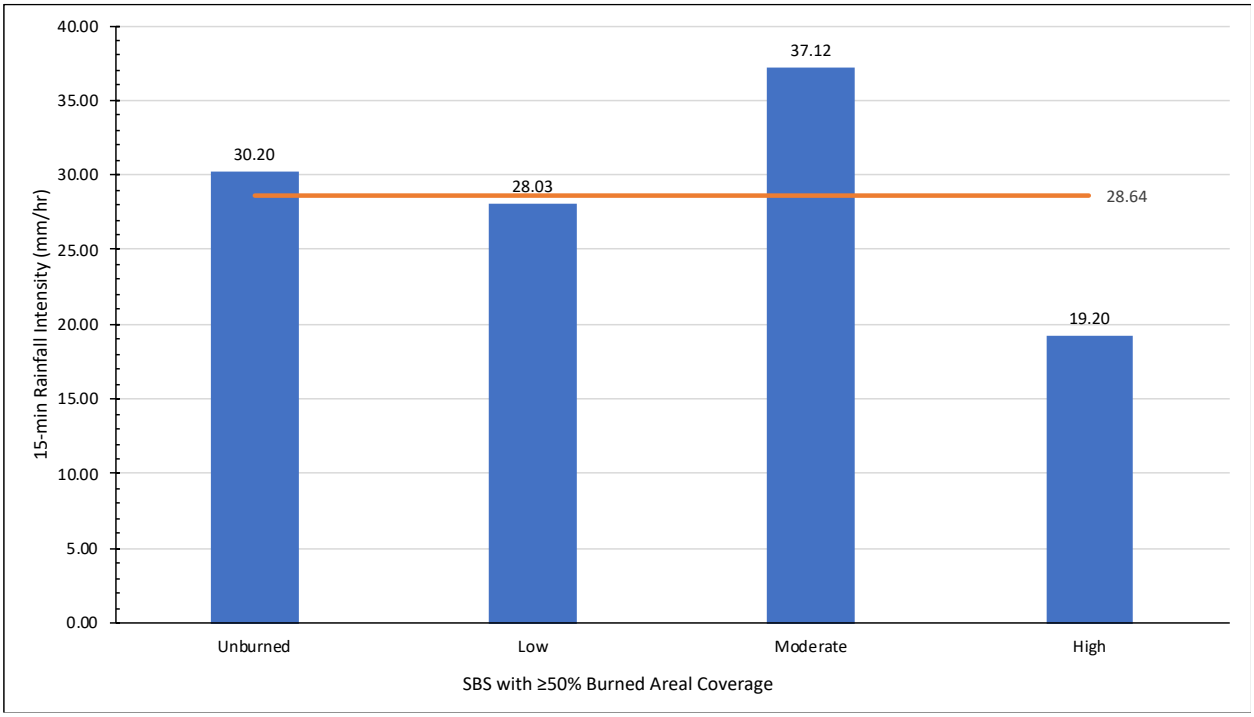

Figure 14. Average peak 15-minute rainfall intensities within debris flow watersheds separated by dominant SBS. Note SBS is considered dominant in a watershed if it equals or exceeds 50% areal coverage of the burned area within the watershed.

4.3 Debris Flows and Total Area Burned

A strong relationship was found between the number of debris flows and the total area burned. When all post-fire debris flows were separated by their respective fires and plotted against total area burned, an R-squared value of 0.85 was obtained (Fig. 15). The Pearson correlation coefficient between the number of debris flows and total area burned (Table 11) was also calculated to be very high (0.92), thus suggesting a strong correlation between the variables.

The number of flows per total area burnt by a fire (flow density) yielded mixed results. The maximum density observed was 1.44 debris flows per square kilometer of area burned, while the least was observed at 0.02 debris flows per square kilometer of area burned (Fig. 16). On average, fires in this study produced a flow density of 0.23. In other words, the region averages one post-fire debris flow per four square kilometers of area burned. A negative Pearson correlation coefficient was then generated between flow density and total area burned (Table 12). This suggests an inverse correlation between the variables.

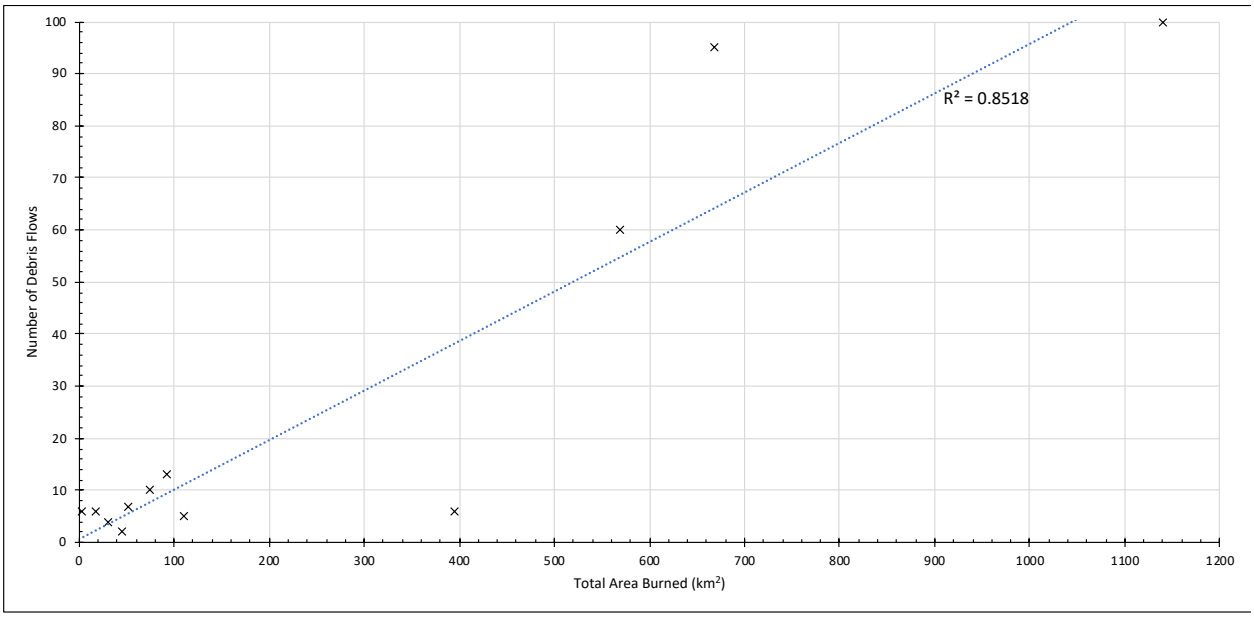

Figure 15. Debris flows and total area burned. Each cross represents a fire, the total number of post-fire debris flows observed within it, and the total area burned by the fire.

Table 11. Pearson correlation coefficient between number of debris flows and total area burned

	Total Area Burned	*Number of Debris Flows*
Total Area Burned	1	
Number of Debris Flows	0.92	1

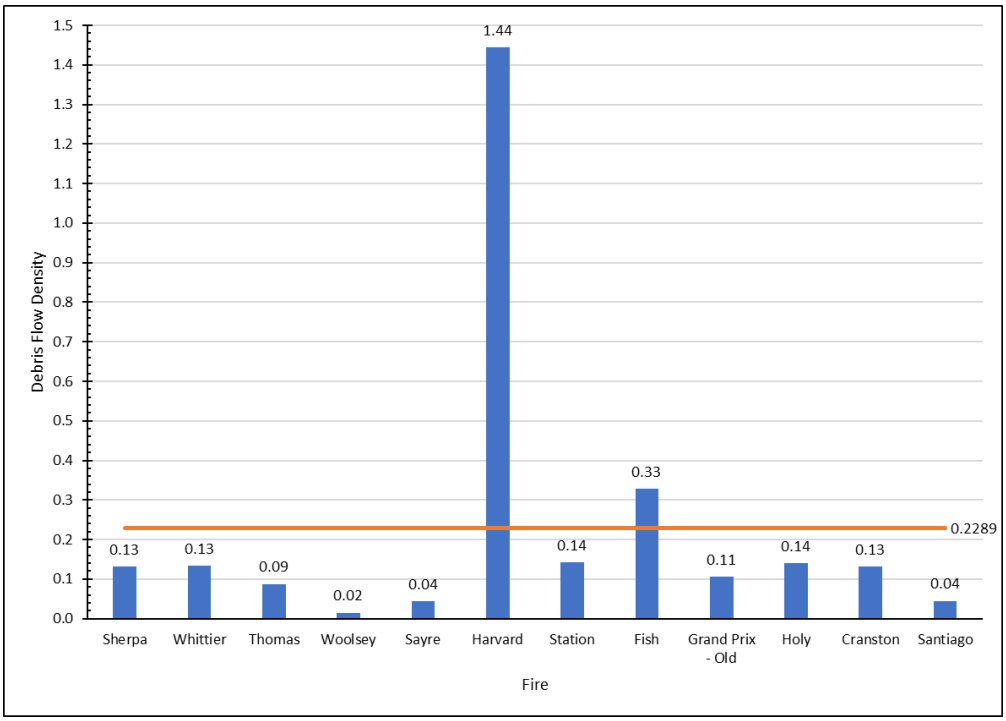

Figure 16. Debris flow density separated by fire. Flow densities generally describe the response over an area. The average value is indicated by the solid line.

Table 12. Pearson correlation coefficient between total area burned and flow density

	Flow Density	*Total Area Burned*
Flow Density	1	
Total Area Burned	-0.27	1

4.4 Debris Flows and Precipitation

Peak 15-minute rainfall intensities recorded for each debris flow varied by fire and region. Average peak intensities ranged from 9.60 mm/hr to 52.98 mm/hr between all twelve fires (Fig. 17). The average peak intensity calculated for all fires was 30.86 mm/hr with mostly fires in the western half of the Transverse Ranges experiencing the highest average intensities. Other fires in the study area largely fall below the intensity average calculated over all fires.

Regional averages highlighted the differences in peak intensity received on average per debris flow watershed (Fig. 18). A high of 44.60 mm/hr was observed in the western Transverse region, which is defined as the part of the range west of the Santa Monica Mountains. The central transverse region was defined as the area from the Santa Monica Mountains to Pomona, CA. The remaining eastern region stretches from Pomona, CA to the eastern-most boundary of the San Bernardino National Forest. All debris flows within the Peninsular Ranges are combined into the northern Peninsular region. Figure 19 visualizes these separations and averages.

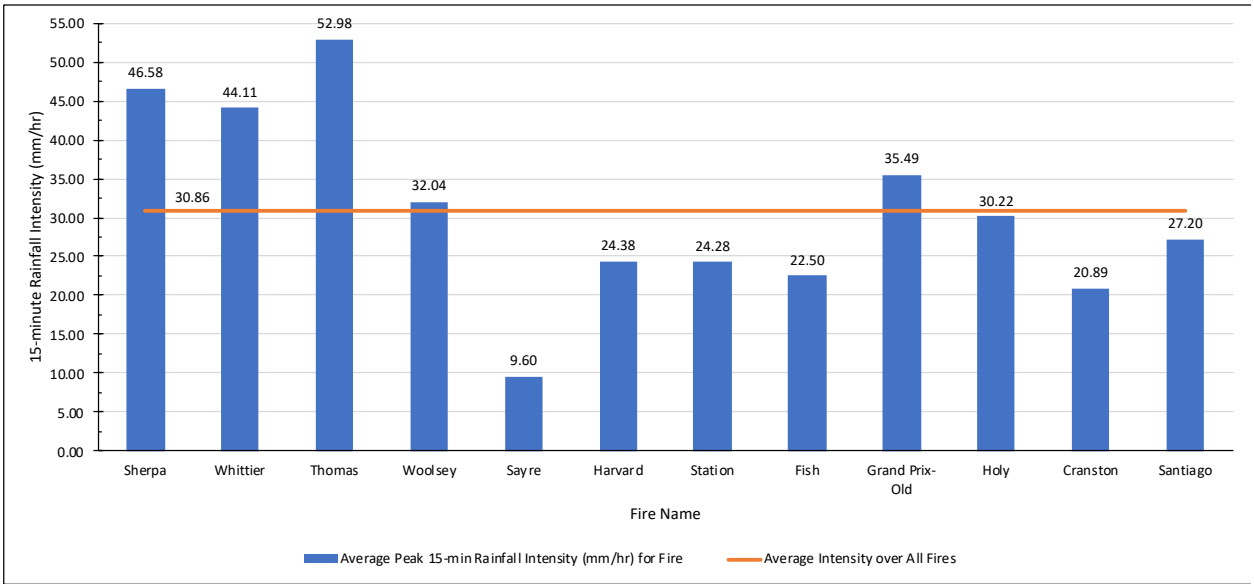

Figure 17. Average peak 15-minute rainfall intensity for each fire. Average values are also labeled according to fire name.

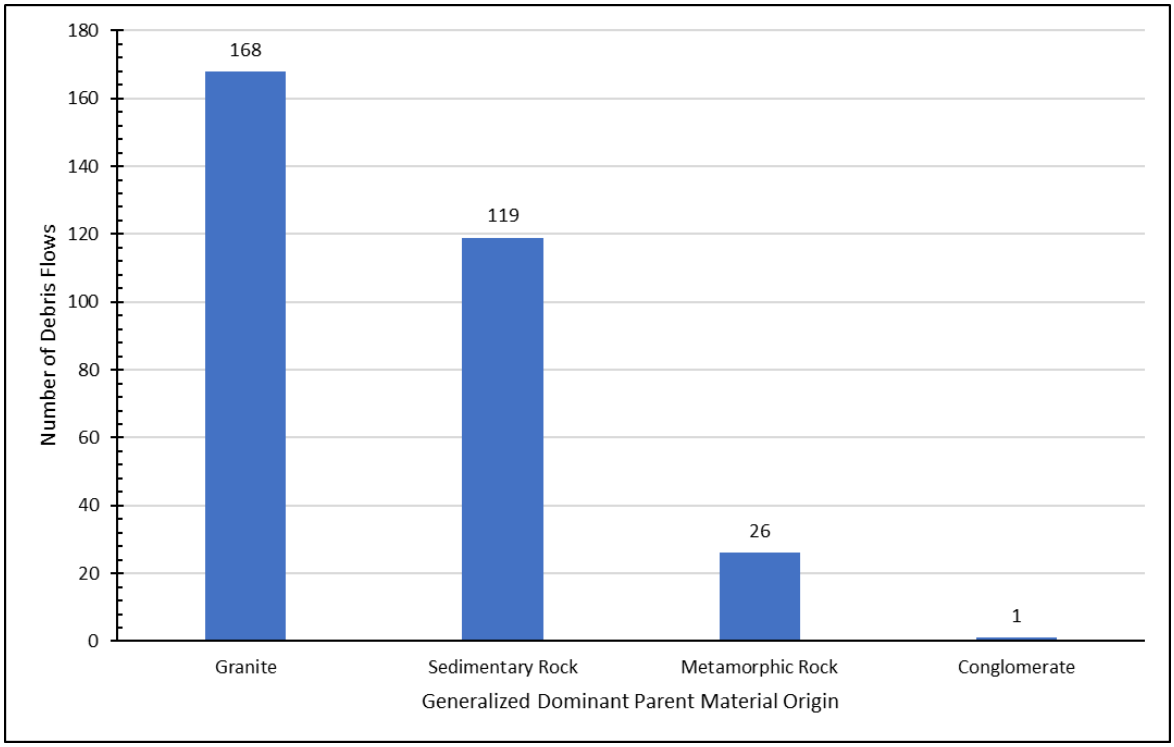

Figure 18. Average peak 15-minute rainfall intensity separated by region. The western Transverse region contains the Sherpa, Whittier, and Thomas fires. The central Transverse region encompasses the Woolsey, Sayre, Harvard, Station, and Fish fires. The eastern Transverse region contains the grand prix-old complex. The northern Peninsular region encompasses the Santiago, Holy, and Cranston fires.

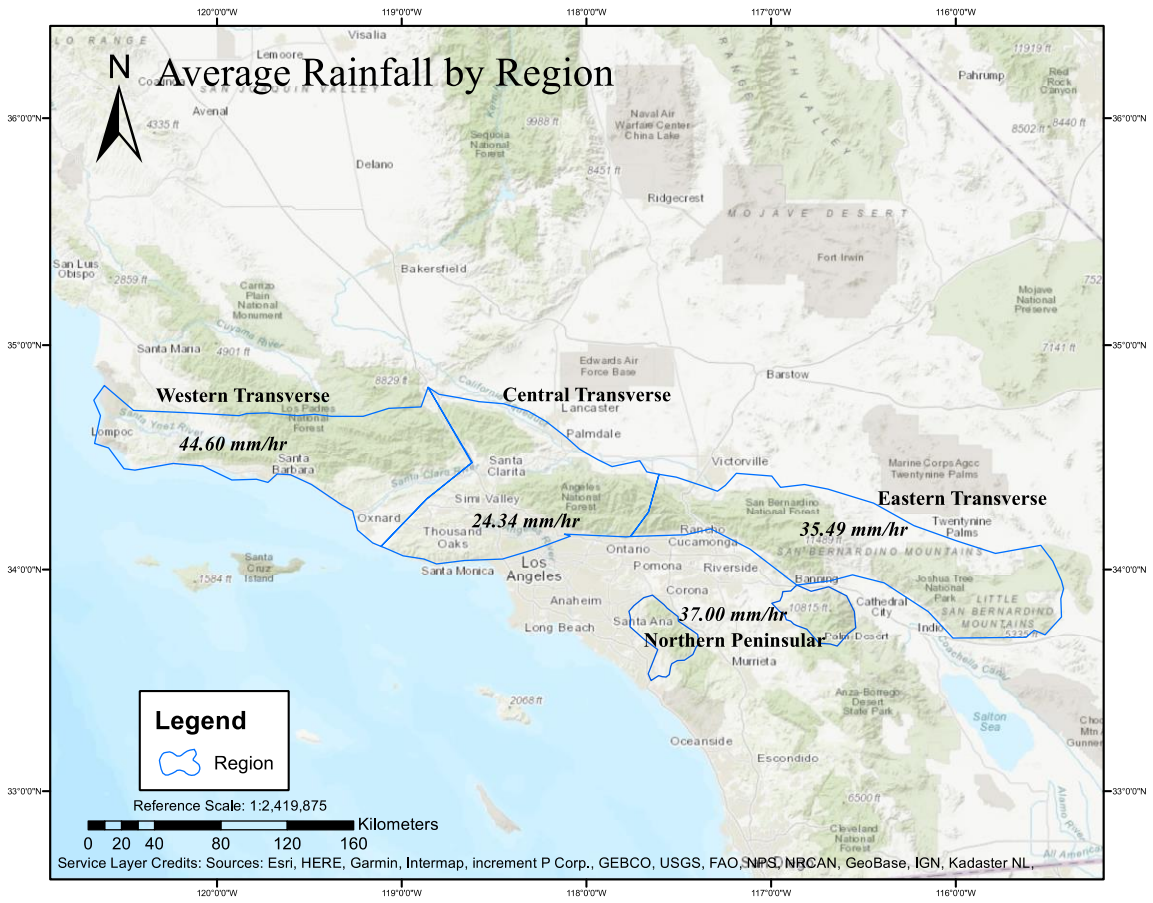

Figure 19. Separations of regions were generally determined off geologic markers such as valleys between mountain ranges. The western boundary of the eastern Transverse region was divided along a ridgeline since the Grand Prix-Old fire burned parts of the Angeles National Forest. Source: Cheung, 2021.

A distribution was generated between the number of flows and peak 15-minute intensity intervals (Fig. 20). Every interval was comprised of 0.99 mm/hr to avoid over-generalization. An average of 4.69 debris flows associated with each interval was calculated. Rainfall intervals (10 to 46 mm/hr) that exceeded the average value also comprised the majority of flows (~77% of the dataset). This translates to a larger number of debris flows being associated with the lower half of the range of rainfall intensity values. This is supported by a negative Pearson's

correlation coefficient that suggests an inverse correlation between the number of debris flows and peak 15-minute rainfall intensity (Table 13).

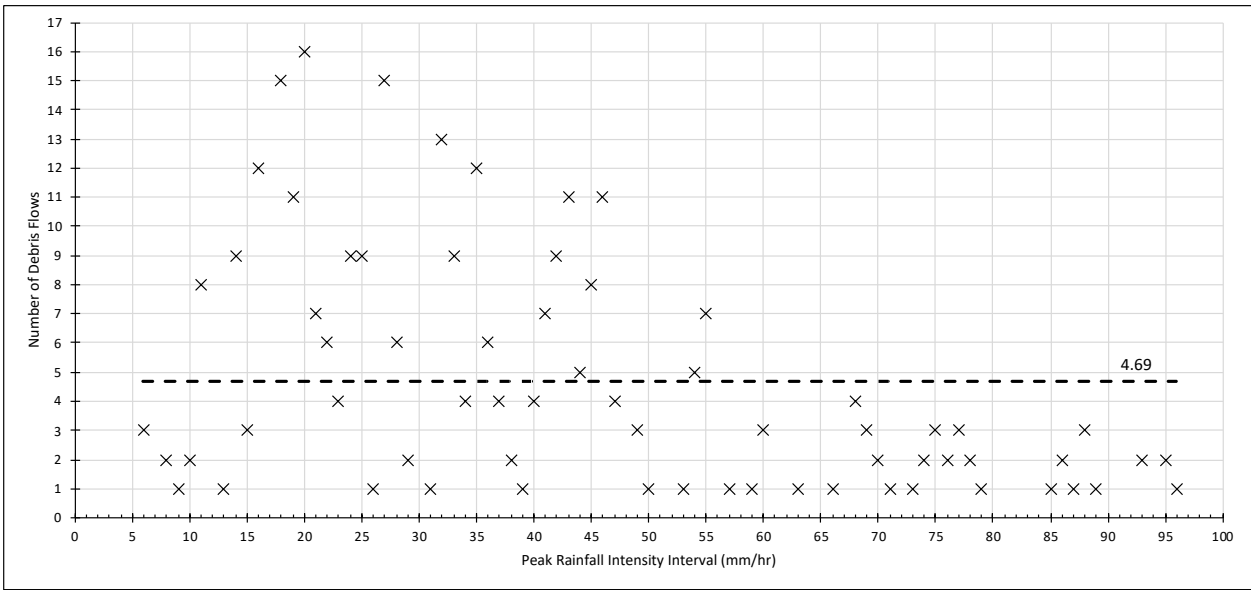

Figure 20. Number of debris flows associated with each interval of peak 15-minute rainfall intensity. Note each value is presented here as a range. For example, an intensity value of 20 mm/hr equates to 20 to 20.99 mm/hr. Any debris flow with a peak 15-minute intensity equal-to or between these values are included in the interval.

Table 13. Pearson correlation coefficient between rain intensity and number of debris flows

	Peak Rainfall Intensity Interval	*Number of Debris Flows*
Peak Rainfall Intensity Interval	1	
Number of Debris Flows	-0.47	1

4.5 Debris Flows and Soils

Within the debris flow watersheds analyzed, eleven dominant soil textures were found. Soil texture descriptions, such as "bedrock," were used where soil textures were not applicable. These were generally locales with little to no soil development. The three most readily occurring textures were found to be bedrock, unweathered bedrock, and weathered bedrock regardless of geologic type (i.e. sedimentary, volcanic, etc.) (Fig. 21). These three textures constituted ~87% (n=273) of all debris flow watersheds in the study, with unweathered bedrock accounting for ~44% (n=137) of all dominant soil textures. Grouped generalizations of these soil textures, again, show a dominance of bedrock soils over a large majority of debris flow watersheds in the dataset (Fig. 22). Loamy soils were the second-most dominant soil texture in the region. Bedrock, unweathered bedrock, and weathered bedrock were combined into the same group because of the generalization process. Various sandy and loamy soils were combined similarly. Decomposed plant material was assigned to a separate, specific group.

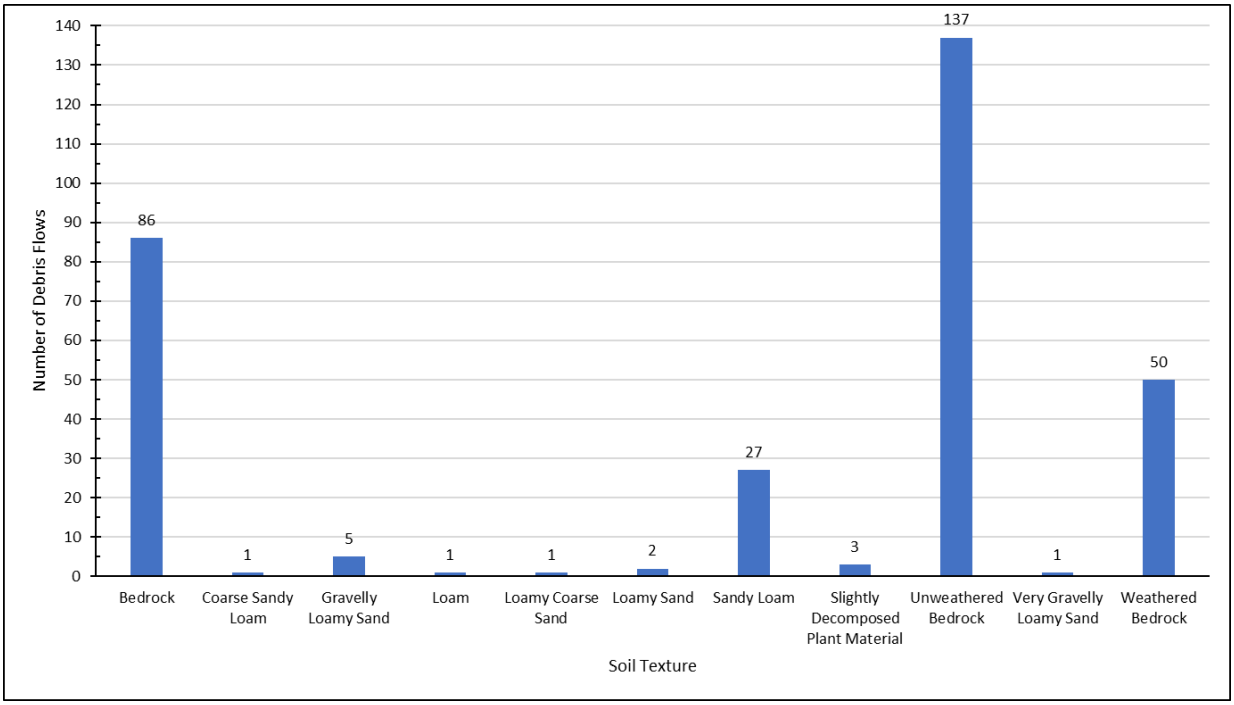

Figure 21. Distribution of soil texture types within debris flow watersheds. Dominant soil texture types were those calculated to populate equal-to or exceed 50% of the burned area within a debris flow watershed.

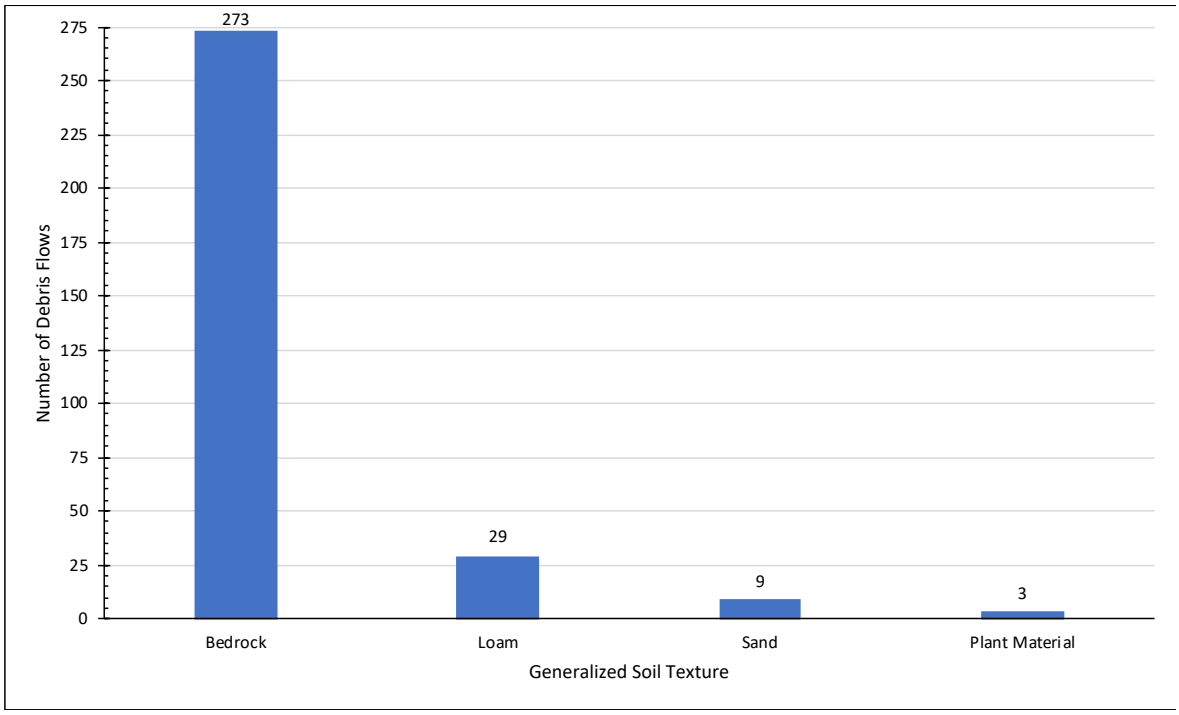

Figure 22. Generalized soil texture distribution. Soil textures with similar characteristics were combined from Figure 16 to create these generalized groups. Loam, sand, and plant material soil textures constituted ~13.06% of debris flows.

Analysis of the dominant parent materials for these soil types, also revealed similar dominant characteristics. Most (~68%) of soil textures were sourced from granite, granodiorite, and sandstone (Fig. 23). Generalizations of all dominant parent materials yielded four basic groups: granitic rock, sedimentary rock, metamorphic rock, and conglomerates (Fig. 24). The granitic rock classification consisted of andesite, anorthosite, diorite, granite, granitoid, and granodiorite. Sedimentary rocks included sandstone, sandstone and shale, sedimentary rock, shale, and siltstone. The metamorphic rock classification contained metamorphic rock, metasedimentary rock, metavolcanics, and schist. Conglomerate-dominated debris flows were given their own group given the difficulty in classifying them within one of the aforementioned

generalizations. It was shown that most (~91%) dominant soils within the dataset originated from granitic and sedimentary rocks, with granitic rocks taking the majority (n=168) of the two parent material types.

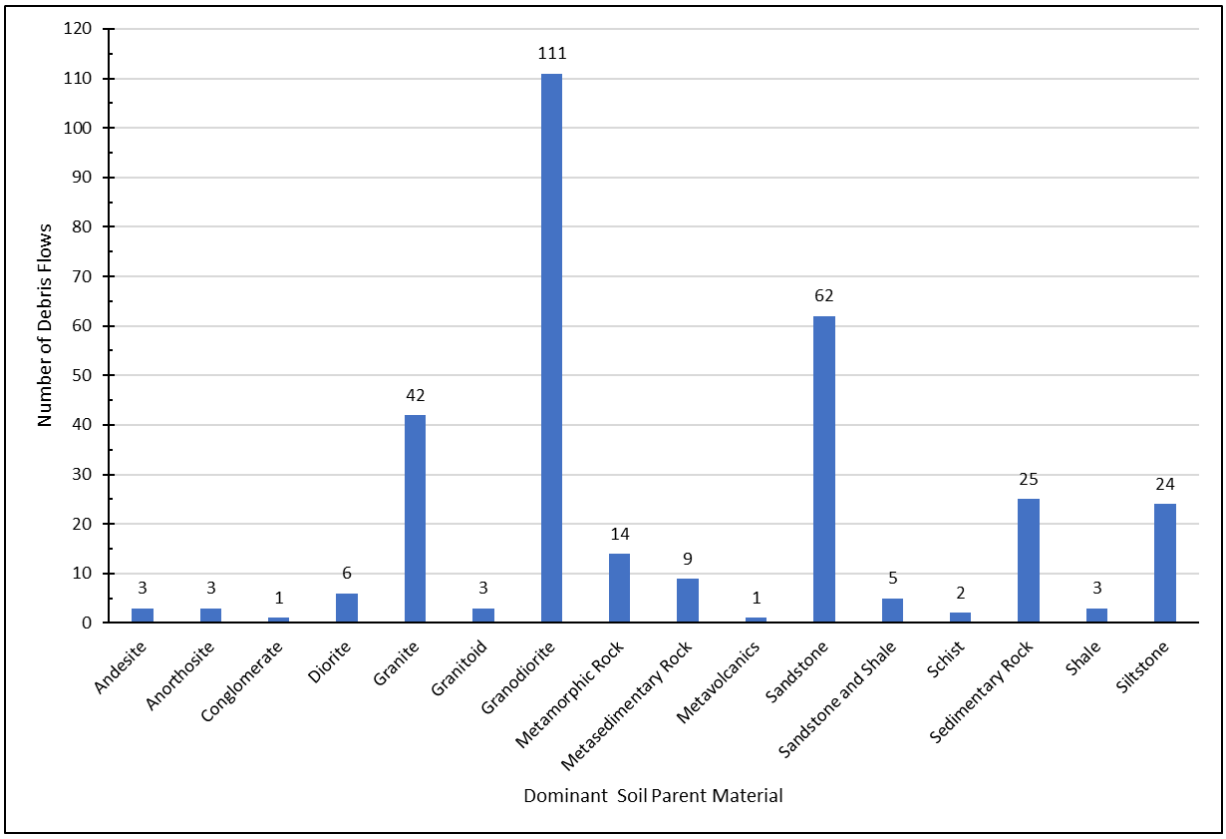

Figure 23. Distribution of flows based off dominant soil texture parent material.

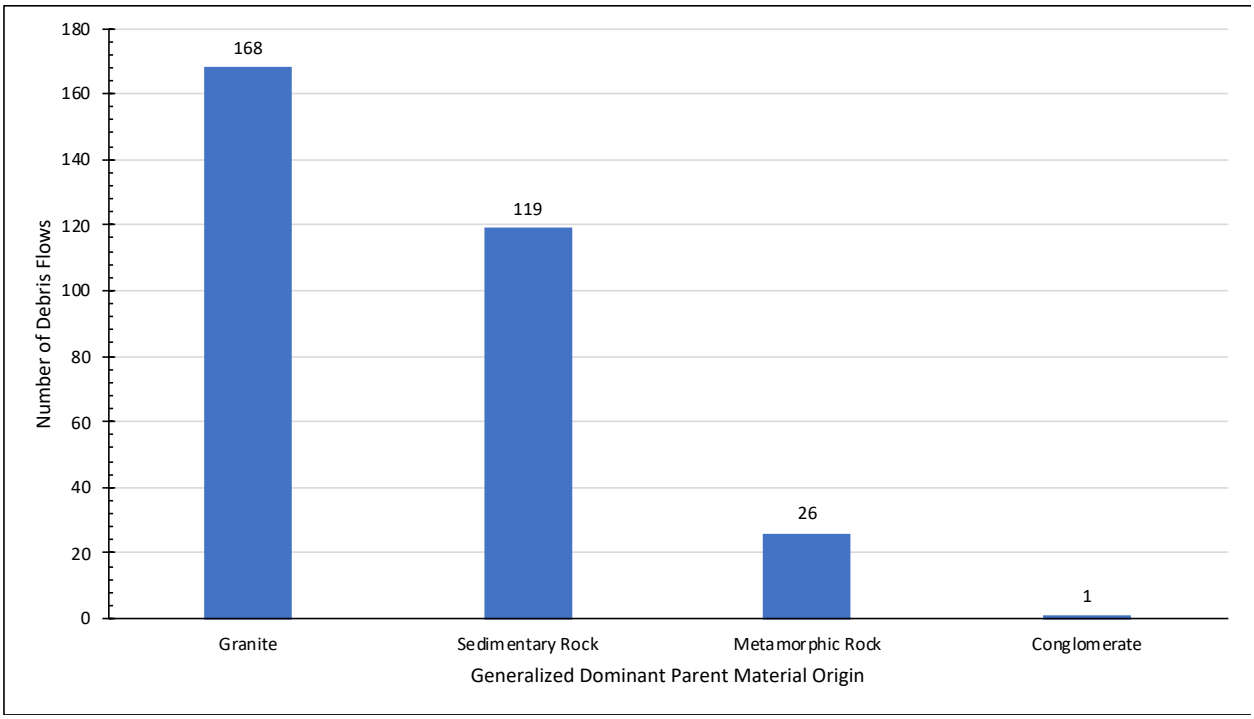

Figure 24. Generalized soil parent material types. Metamorphic rock and conglomerate classifications only consisted of 8.60% of debris flows in the dataset.

When dominant SBS was combined with generalized soil descriptions the number of debris flows was heavily concentrated within a single SBS classification (Fig. 25 and Fig. 26). The combination of SBS with generalized soil textures from Figure 25 showed that most (72.93%) debris flows in the study possessed soils dominated by moderate SBS and of bedrock texture. This was followed by debris flows sourced from loamy soils (7.32%) with a dominant moderate SBS classification. A similar analysis that combined SBS and soil texture parent material provided similar results (Fig. 26). Most (~84%) debris flows in the study originated from dominant moderate SBS watersheds regardless of soil texture parent material. Within this group, ~43% of all debris flows (n=136) occurred from dominant moderate SBS watersheds with granite as the dominant soil texture parent material. This was followed closely by debris flows

with dominant moderate SBS watersheds and sedimentary rocks as the dominant soil texture parent material (n=104).

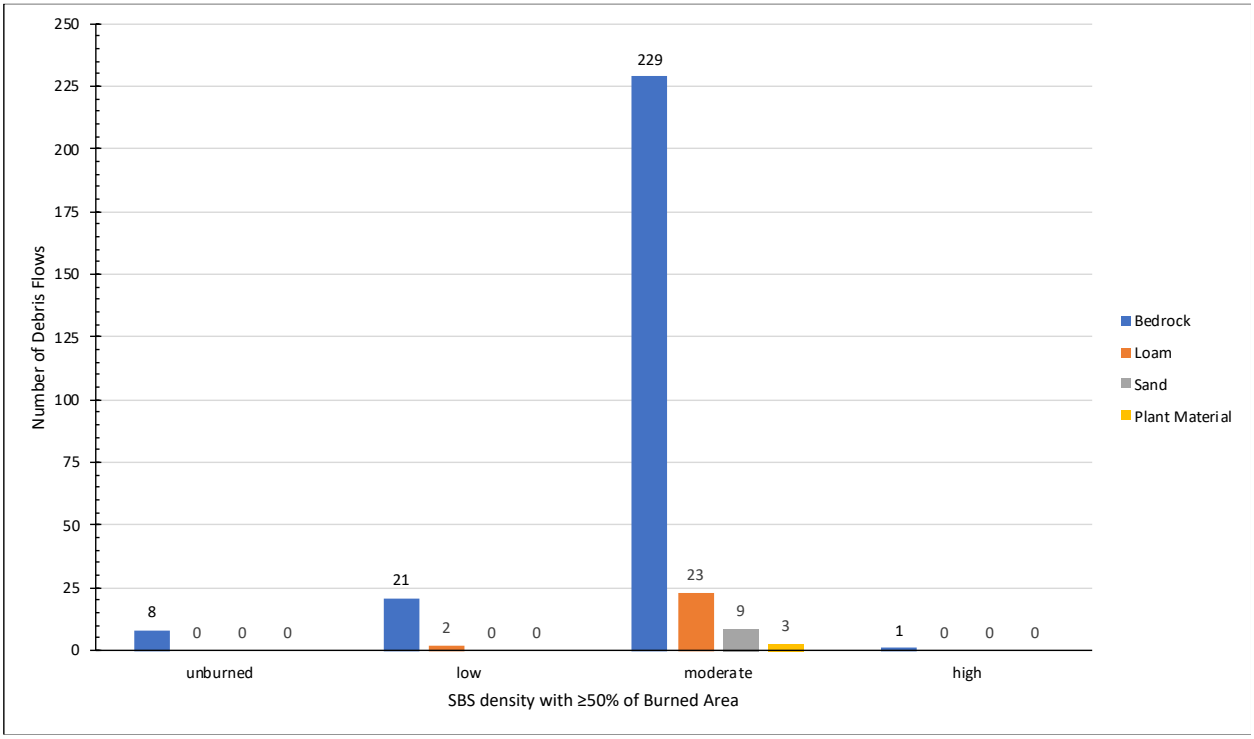

Figure 25. Debris flow distribution over various SBS classifications. This was further divided into general soil texture classes generated from Figure 17.

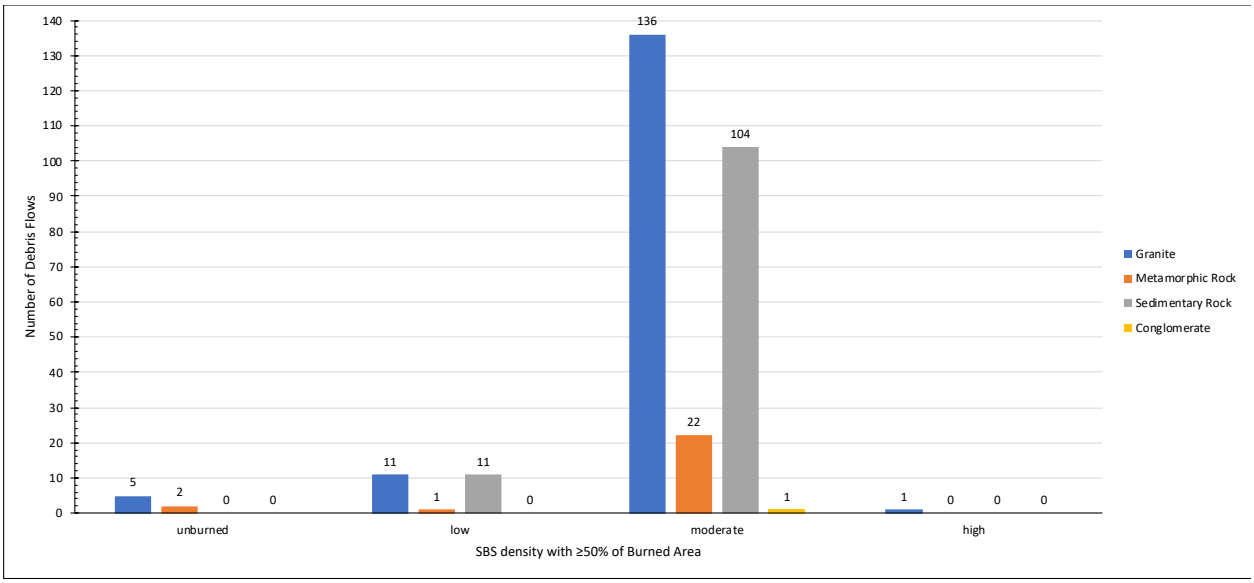

Figure 26. Debris flow distribution over various SBS classifications divided by generalized soil texture parent material generated in Figure 19.

5. DISCUSSION

General statistics of all debris flows in the dataset corroborates with previous work conducted by other studies. Most debris flow watersheds drain in a southerly direction, which was a similar observation made by Rengers et al. (2020) in their analysis of post-fire shallow landslides in southern California. This is likely because these watersheds face towards the Pacific Ocean, which is the source of the majority of precipitation in the region (Hoell et al., 2016; Jong et al., 2016). El Niño Southern Oscillations and narrow cold-frontal rainbands trend west to east towards land as demonstrated by Oakley et al. (2018). When these westerly or southwesterly storms encounter southern California, they may be subjected to orographic forcing, resulting in a deluge of rainfall on these seaward slopes (Valenzuela and Kingsmill, 2015). The noticeable increase in number of debris flows associated with slope intervals greater than 20 degrees is very similar to findings by Cannon et al. (2010) and those employed by the USGS post-fire debris flow prediction model (Staley et al., 2016). The size of watersheds and area burned within each watershed both seemed to demonstrate the ability of both "large" and "small," "lightly burned" and "extensively burned" watersheds to produce responses and that debris flows are not necessarily constrained to specific watershed area or burned area thresholds.

Analyses between SBS and the number of debris flows suggested a strong relationship between the two variables (Fig. 27). The tendency for most debris flows to have most of their burned area associated with moderate SBS rates could possibly be attributed to the natural propensity for fires to burn more soils at moderate SBS levels than higher ones. Positive and negative correlations between SBS density and number of debris flows could possibly be explained by this phenomenon. Negative correlations might be attributed to the overall rarity of

unburned and high SBS densities within a fire footprint when compared to moderate and low SBS densities. A higher number of debris flows were associated with the low SBS density classification between SBS density values of 0 and 0.3 (Fig. 11). This illustrates how numerous debris flow watersheds also have more of their areas burned at low SBS than unburned and high SBS classification. The speculation regarding natural fire patterns affecting SBS densities may also be bolstered by the Tukey's HSD output where density means between most SBS classifications were found to be statistically different from one another, except between unburned and high SBS densities.

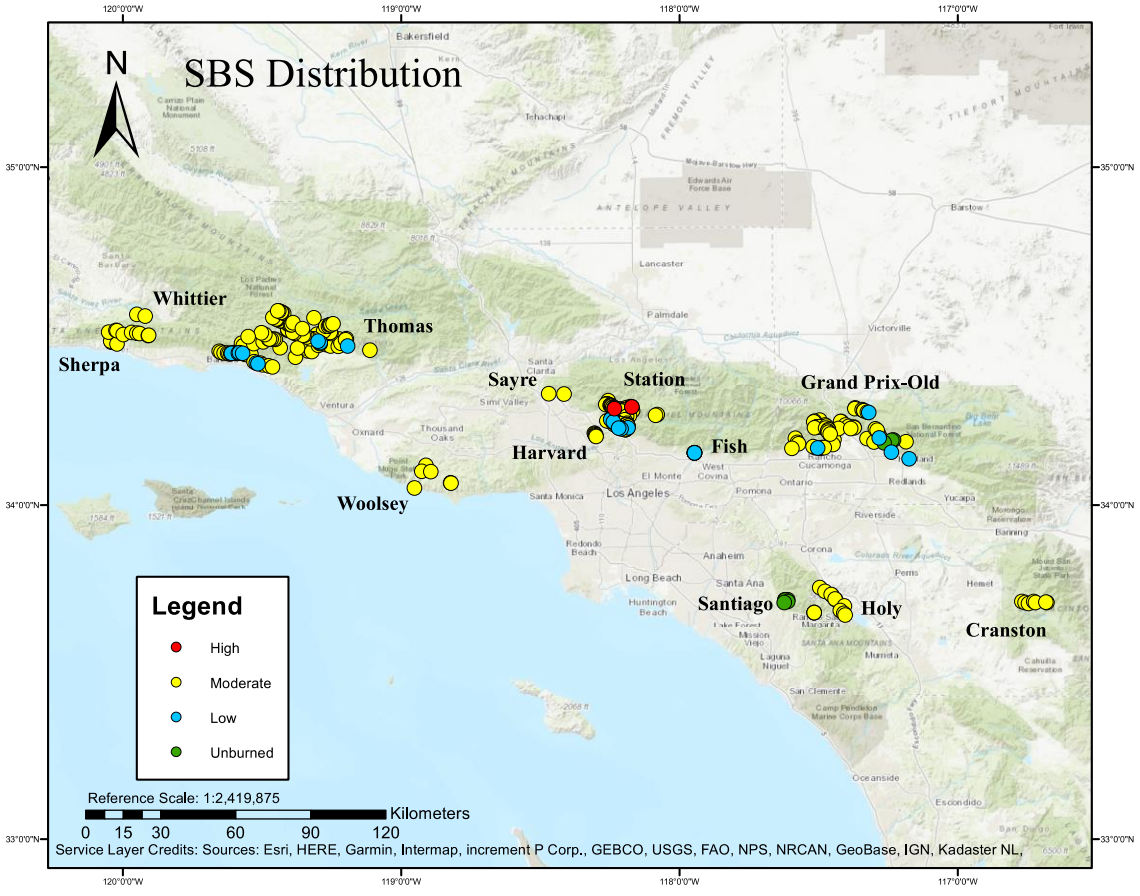

Figure 27. Distribution of debris flows based off dominant SBS density. Each point represents a debris flow observation and the SBS density that characterizes most of its watershed. Fire names are labeled for reference. Source: Cheung, 2021.

A similar comparison replacing SBS density with SBS areal coverage provided less discernable results. Negative Pearson correlation coefficients between all SBS classification areas and number of debris flows suggest that debris flow occurrence may not be directly related to area burned under various severities. As demonstrated by SBS densities, the moderate SBS areal coverage average seemed to statistically differ from unburned, low, and high SBS area coverage means. This suggests that debris flow occurrence in the region is also somewhat dependent upon the amount of area burned to a moderate SBS classification.

The analysis between SBS and rainfall provided insight into how each SBS may respond to peak 15-minute rainfall intensities. Watersheds with predominantly unburned and low SBS classifications hovered around the mean while moderate SBS watersheds experienced higher peak 15-min intensities on average. This could be attributed to the ubiquity of debris flows with moderate SBS. The uneven number of debris flows within each category possibly altered these results. It is possible that average rainfall intensities should actually be higher in debris flow watershed dominated by low and unburned SBS classifications since soil material is less erodible than higher severities (Parsons et al., 2010).

Correlations between the number of debris flows and total area burned by a fire yielded strong results. A high correlation coefficient suggests that as total areas burned by fires increases, the number of debris flows will increase in tandem. Separating debris flows by fire yielded flow densities that negatively correlated with total area burned by fires. This suggests that as total area burned increases, the density of debris flows will not necessarily increase in responses. It is believed that larger fires increase the area available for post-fire debris flow generation but may not experience as high a flow density than smaller fires. From these results,

larger fires seem to have more debris flows than smaller fires, but lower flow densities given the area burned is much larger for large fires.

Precipitation results attached to debris flows mirrored earlier work (i.e. Staley et al., 2020). Regional peak 15-minute rainfall intensity means were found to differ by region. Larger peak rainfall intensities in western regions could possibly be linked to their proximity to the ocean as discussed by Valenzuela and Kingsmill (2015). Similar to the findings of Staley et al. (2020), the number of flows were mostly concentrated in lower rainfall intensities (Fig. 15). This corroborates their claim that debris flows are largely associated with precipitation events with one or two-year recurrence intervals. A negative correlation coefficient between peak 15-minute rainfall intensities and number of debris flows suggests that the two variables are not directly related, however this negative value may be explained by the general rarity of high-intensity events. This natural rarity would thus be associated with less debris flows.

The number of debris flows were found to be highly reliant on local soil characteristics. A large majority of flows occurring on bedrock soil textures suggest the high erodibility of these exposed areas, weathered or otherwise. The dominant parent material of these soil textures reflected the local geology of the region, granitic and sedimentary rock. When soil textures were paired with their dominant SBS density, it was found that most (~73%) debris flow watersheds occurred on bedrock textures at moderate SBS. After soil texture parent materials were paired with dominant SBS densities, it was found that most (76%) debris flows originated from moderately burned soils that stem from granitic and sedimentary rocks. These results not only reflect the ubiquity of these soil textures and their parent material in the area, but the immense contribution moderately burned soils seem to have over debris flow occurrence.

A lack of publicly available data was a major limitation to this study. The general lack of data in regard to debris flow locations, timing, and accompanying SBS spatial datasets was a factor in determining the accuracy of these findings. Of the data that was compiled, there is a general lack of consistency in post-fire monitoring for post-fire debris flows. Different fires were monitored to different degrees. Some fires, especially those that burned in chiefly backcountry areas, only possessed observations for a small fraction of their burned extent given limited routes of physical access. Select fires possessed multiple observations for the same watershed, while others only received a single observation per watershed. This is most likely because of limited documentation efforts and not the inexistence of more than one event within a watershed. In fact, southern Californian studies such as Tang et al. (2019) illustrate the ability for a drainage to experience multiple responses within a single rainstorm. SBS datasets were also largely limited to USFS lands since BAER teams, the creators of SBS spatial data, are usually only deployed to USFS lands. As a result, NPS lands in southern California and State lands generally lack older SBS data. In more recent years, these agencies commonly request BAER teams for SBS products, but they have yet to be made readily, publicly available. Few debris flows in the dataset possessed predominantly high SBS classifications in their watersheds. This limits the analysis of a comparison of their characteristics with other SBS classifications. Satellite imagery provided by Planet Team (2017) is not publicly available but may be more affordable for researchers to employ compared to other competitors. The general difficulty with attaching triggering rainfall to observations are based off a lack of temporal debris flow occurrence data. This limited this study to only identifying peak 15-minute rainfall intensities. Further, rainfall data was found to be highly decentralized, which made it difficult for precipitation data to be readily, publicly accessed for all areas within the study area. This is

largely attributed to agencies allowing access to hourly rainfall records, which is often the finest temporal resolution offered to the public through online platforms.

Available datasets also posed their own complications. Precipitation data was generally recorded with varying types of tipping bucket gauge stations with varying levels of precision. SBS datasets are provided at a coarse 30m spatial resolution and are naturally prone to generalization. There is a possibility that "field-verified" areas may not actually be representative of other areas within the fire that exhibited similar spectral signatures. Slope maps generated from DEMs gathered for the area may be inaccurate (i.e., recent landslides causing steep reliefs, channel scouring, etc.) if the DEM was not produced recently. Much of the soil dataset was also lacking data for various categories, thus limiting more detailed analyses of soil properties. The satellite imagery employed for this study possessed a spatial resolution of 3m, which makes the identification of small erosion features (rills) and small scouring events more difficult.

Processing the dataset was also a concern. Interpolating rainfall using the IDW method may have given wrong peak 15-minute intensities over an area. Attaching SBS spatial data to debris flow watersheds might have removed some pixels from the SBS spatial dataset, thus leading to a miscalculation of SBS within a watershed. If this error occurred, it is believed the effect of the issue would have been negligible. All areas calculated in ArcMap® might have lacked precision since they were calculated with 30m pixels. The same concern was attributed to 10m DEMs used to delineate watershed boundaries. Dominant soil textures calculated within ArcMap® may not have been the source of the debris flow matrix. This was a large concern, so the 3 most populous soil textures were included in the characterization process instead of solely

considering the major soil unit. Choosing the most representative pre-fire and post-flow satellite imagery for scour identification was dependent upon available data and satellite paths.

6. CONCLUSION

Changing fire regimes, products of a changing climate, pose numerous challenges for human society. Previous hypotheses of increasing burn severity (Potter, 2017; Sommerfeld et al., 2018), annual area burned (Vose et al., 2012), and large forest fire incidents (Wuebbles et al., 2017; Yue et al., 2013) have come to fruition in California within the last few years (CALFIRE), 2018) with no end in sight. Burned soils exposed to the elements lacking structural integrity are commonly eroded in the form of post-fire debris flows. As a part of an intricate sub-system of nature that is post-fire erosion, post-fire debris flow patterns were found in this study to respond to these changing fire regimes.

Analyses of recent (2001-2018) post-fire debris flows presented implications for future debris flow occurrence in the southern Californian region. Most debris flows (~84%) in the dataset were found to originate from watersheds with soils burned at moderate severity. The number of debris flows per fire increased with the total area burnt, however flow density within a fire was not found to be directly correlated with the total area burned by a fire. More debris flow watersheds were associated with at least 20 to 45-degree slopes than lower gradients. Average peak 15-minute rainfall intensities were observed to be the highest in the western region of the Transverse Ranges. A majority (~87%) of debris flows originated from watersheds dominated by bedrock lithology. When soil textures were analyzed alongside dominant SBS classifications, it was found that most (~73%) debris flows originated from bedrock burned at moderate severities. Parent materials for dominant soil textures (including bedrock) were found to mostly (~91%) originate from granitic and sedimentary rocks. An analysis of parent materials and dominant SBS classifications showed another majority (~75%) of flows with dominant soil

texture parent materials of granitic and sedimentary origins burned at predominantly moderate severity. From these findings, it is suggested that, if fires continue to increase in size, occur on slopes of at least 20 degrees, and predominantly burn bedrock of granitic or sedimentary origins to at least a moderate severity, there should be a noticeable increase in the number of post-fire debris flows in the region. Hillslope processes will likely respond to changing fire regimes, and thus a changing climate in the near future given the last 20 years of data. Further, this finding affirms the prediction made by Sankey et al. (2017) of increased sedimentation of watersheds in the western USA over the coming century .

Continued exploration of this topic is needed to further develop this conclusion as it is imperative to increase human resiliency in light of future uncertainty. Novel techniques are needed to better elucidate differences in triggering conditions between debris flow watersheds with differing dominant SBS classifications. SBS spatial datasets should be regularly produced regardless of jurisdiction to prevent biased analyses of only USFS lands. Increased data collection could further test these findings for accuracy and better advise natural resource managers. Remote sensing approaches should also be further developed to identify post-fire debris flows in rugged terrains. Robust documentation of debris flows would provide scientists with a stronger understanding of optimal conditions for debris flow generation in response to climate change. Finally, it is critical for fire ecologists, hydrologists, geomorphologists, and the public at large to communicate and collaborate in post-fire hazard planning and mitigation. Local communities will have to find a way to respond not only to worsening fire regimes, but heightened risks of subsequent erosive hazards as well.

REFERENCES

Balch, J.K., Bradley, B.A., Abatzoglou, J.T., Nagy, R.C., Fusco, E.J., Mahood, A.L., 2017. Human-started wildfires expand the fire niche across the United States. Proc. Natl. Acad. Sci. U. S. A. 114, 2946–2951. https://doi.org/10.1073/pnas.1617394114

Bellamy, K., Beebe, J.T., Saunderson, H.C., 1992. Erosion and sediment transport monitoring programmes in river basins. IAHS Publ.

Beverage, J.P., Culbertson, J.K., 1964. Hyperconcentrations of suspended sediment. Am. Soc. Civ. Eng. J. Hydraul. Div. 90, 117–128.

Bray, M.J., Carter, D.J., Hooke, J.M., 1995. Littoral cell definition and budgets for central southern England. J. Coast. Res. 11, 381–400.

California Department of Forestry and Fire Protection(CALFIRE), 2018. 2018 wildfire activity statistics. Sacramento, CA.

Cannon, S.H., Gartner, J.E., Rupert, M.G., Michael, J.A., Rea, A.H., Parrett, C., 2010. Predicting the probability and volume of postwildfire debris flows in the intermountain western United States. Bull. Geol. Soc. Am. 122, 127–144. https://doi.org/10.1130/B26459.1

Cannon, S.H., Gartner, J.E., Wilson, R.C., Bowers, J.C., Laber, J.L., 2008. Storm rainfall conditions for floods and debris flows from recently burned areas in southwestern Colorado and southern California. Geomorphology 96, 250–269. https://doi.org/10.1016/j.geomorph.2007.03.019

Cannon, S.H., Kirkham, R.M., Parise, M., 2001. Wildfire-related debris-flow initiation processes, Storm King Mountain, Colorado. Geomorphology 39, 171–188. https://doi.org/10.1016/S0169-555X(00)00108-2

Cleetus, R., Mulik, K., 2014. Playing with fire: how climate change and development patterns are contributing to the soaring costs of western wildfires (2014).

Costa, J.E., 1988. Rheologic, geomorphic, and sedimentologic differentiation of water floods, hyperconcentrated flows, and debris flows, in: Baker, V.R., Kochel, R.C., Patton, P.C. (Eds.), Flood Geomorphology. Wiley-Intersciences, New York, pp. 113–122.

Doerr, S.H., Shakesby, R.A., Blake, W.H., Chafer, C.J., Humphreys, G.S., Wallbrink, P.J., 2006. Effects of differing wildfire severities on soil wettability and implications for hydrological response. J. Hydrol. 319, 295–311. https://doi.org/10.1016/j.jhydrol.2005.06.038

Emmett, W.W., 1970. The hydraulics of overland flow on hillslopes. Dynamic and descriptive studies of hillslopes.

Handwerger, A.L., Fielding, E.J., Huang, M.H., Bennett, G.L., Liang, C., Schulz, W.H., 2019. Widespread initiation, reactivation, and acceleration of landslides in the northern California Coast Ranges due to extreme rainfall. J. Geophys. Res. Earth Surf. 124, 1782–1797. https://doi.org/10.1029/2019JF005035

Highland, L.M., Ellen, S.D., Christian, S.B., Brown III, W.M., 1997. Debris-Flow Hazards in the United States.

Hoell, A., Hoerling, M., Eischeid, J., Wolter, K., Dole, R., Perlwitz, J., Xu, T., Cheng, L., 2016. Does El Niño intensity matter for California precipitation? Geophys. Res. Lett. 43, 819–825. https://doi.org/10.1002/2015GL067102

Hubbert, K.R., Preisler, H.K., Wohlgemuth, P.M., Graham, R.C., Narog, M.G., 2005. Prescribed burning effects on soil physical properties and soil water repellency in a steep chaparral watershed, southern California, USA. Geoderma. 130, 284-298. https://doi.org/10.1016/j.geoderma.2005.02.001

Iverson, R.M., 1997. The physics of debris flows. Rev. Geophys. 35, 245–296. https://doi.org/10.1029/97RG00426

Jahns, R.H., 1954. Geology of the Pennsular Range province, southern California and Baja California, in: Geology of the natural provinces. California Institute of Technology, pp. 29–52.

Jennings, C.W., 1959. Geologic map of California, Santa Maria sheet, California.

Jennings, C.W., Strand, R.G., 1969. Geologic map of California, Los Angeles sheet, California.

Johnson, C.G., Kokelaar, B.P., Iverson, R.M., Logan, M., Lahusen, R.G., Gray, J.M.N.T., 2012. Grain-size segregation and levee formation in geophysical mass flows. J. Geophys. Res. Earth Surf. 117. https://doi.org/10.1029/2011JF002185

Johnson, P.A., McCuen, R.H., Hromadka, T. V., 1991. Magnitude and frequency of debris flows. J. Hydrol. 123, 69–82. https://doi.org/10.1016/0022-1694(91)90069-T

Jong, B.T., Ting, M., Seager, R., 2016. El Niño's impact on California precipitation: Seasonality, regionality, and El Niño intensity. Environ. Res. Lett. 11, 54021. https://doi.org/10.1088/1748-9326/11/5/054021

Kean, J.W., Staley, D.M., Cannon, S.H., 2011. In situ measurements of post-fire debris flows in southern California: Comparisons of the timing and magnitude of 24 debris-flow events with rainfall and soil moisture conditions. J. Geophys. Res. 116, F04019. https://doi.org/10.1029/2011JF002005

Kean, J.W., Staley, D.M., Lancaster, J.T., Rengers, F.K., Swanson, B.J., Coe, J.A., Hernandez, J.L., Sigman, A.J., Allstadt, K.E., Lindsay, D.N., 2019. Inundation, flow dynamics, and damage in the 9 January 2018 Montecito debris-flow event, California, USA: Opportunities and challenges for post-wildfire risk assessment. Geosphere 15, 1140-1163.

https://doi.org/10.1130/GES02048.1

Keane, R.E., Agee, J.K., Fulé, P., Keeley, J.E., Key, C., Kitchen, S.G., Miller, R., Schulte, L.A., 2008. Ecological effects of large fires on US landscapes: benefit or catastrophe? A. Int. J. Wildl. Fire 17, 696–712. https://doi.org/10.1071/WF07148

Keeley, J.E, 2008. Fire intensity, fire severity and burn severity: A brief review and suggested use. Int. J. Wildl. Fire 18, 116–126.

Keeley, J.E., 2008. Fire, in: Encyclopedia of ecology, five-volume set. Elsevier Inc., pp. 1557–1564. https://doi.org/10.1016/B978-008045405-4.00496-1

Lentile, L.B., Holden, Z.A., Smith, A.M.S., Falkowski, M.J., Hudak, A.T., Morgan, P., Lewis, S.A., Gessler, P.E., Benson, N.C., 2006. Remote sensing techniques to assess active fire characteristics and post-fire effects. Int. J. Wildl. Fire 15, 319–345. https://doi.org/10.1071/WF05097

Littell, J.S., McKenzie, D., Peterson, D.L., Westerling, A.L., 2009. Climate and wildfire area burned in western U.S. ecoprovinces, 1916–2003. Ecol. Appl. 19, 1003–1021. https://doi.org/10.1890/07-1183.1

Lukashov, S.G., Lancaster, J.T., Oakley, N.S., Swanson, B.J., 2019. Post-fire debris flows of 9 January 2018, Thomas Fire, southern California: Initiation areas, precipitation and impacts. 7th Int. Conf. Debris-Flow Hazards Mitig.

McCoy, S.W., 2015. Infrequent, large-magnitude debris flows are important agents of landscape change. Geology 43, 463–464. https://doi.org/10.1130/focus052015.1

Minnich, R.A., 2007. Introduction to the distribution and species composition of the region's forest, in: Barbour, M. (Ed.), terrestrial vegetation of California. California Scholarship Online, pp. 502–538.

Moody, J.A., Ebel, B.A., Nyman, P.C., Martin, D.A., Stoof, C.R., McKinley, R.F., 2016. Relations between soil hydraulic properties and burn severity. Int. J. Wildl. Fire 25, 279–293. https://doi.org/10.1071/WF14062

Moody, J.A., Martin, D.A., 2001. Initial hydrologic and geomorphic response following a wildfire in the Colorado Front Range. Earth Surf. Process. Landforms 26, 1049–1070. https://doi.org/10.1002/esp.253

Morton, D.M., Yerkes, R.F., 1987. Recent reverse faulting in the Transverse Ranges, California.

Mowery, M., Read, A., Johnston, K., Wafaie, T., 2019. American Planning Association planning advisory service creating great communities for all: Planning the wildland-urban interface.

National Weather Service (NWS), 1995. Annual average precipitation (inches) Southern California.

Neary, D.G., Ryan, K.C., DeBano, L.F., 2008. Wildland fire in ecosystems: effects of fire on soils and water.

Oakley, N.S., Cannon, F., Munroe, R., Lancaster, J.T., Gomberg, D., Ralph, F.M., 2018. Brief communication: Meteorological and climatological conditions associated with the 9 January 2018 post-fire debris flows in Montecito and Carpinteria, California, USA. Nat. Hazards Earth Syst. Sci. 18, 3037–3043. https://doi.org/10.5194/nhess-18-3037-2018

Parsons, A., Robichaud, P.R., Lewis, S.A., Napper, C., Clark, J.T., 2010. Field guide for mapping post-fire soil burn severity.

Peterson, D.L., Littell, J.S., 2014. Risk Assessment for Wildfire in the Western United States. https://doi.org/10.1029/2011JG001695

Planet Team, 2017. Planet application program interface: In space for life on Earth.

Potter, C., 2017. Fire-climate history and landscape patterns of high burn severity areas on the

California southern and central coast. J. Coast. Conserv. 21, 393–404. https://doi.org/10.1007/s11852-017-0519-3

Reid, L.M., Dunne, T., 2016. Sediment budgets as an organizing framework in fluvial geomorphology. Tools Fluv. Geomorphol. 357–379. https://doi.org/https://doi.org/10.1002/9781118648551

Rengers, F.K., McGuire, L.A., Oakley, N.S., Kean, J.W., Staley, D.M., Tang, H., 2020. Landslides after wildfire: initiation, magnitude, and mobility. Landslides 17, 2631–2641. https://doi.org/10.1007/s10346-020-01506-3

Robichaud, P.R., Beyers, J.L., Neary, D.G., 2000. Evaluating the effectiveness of postfire rehabilitation treatments.

Rogers, T.H., 1967. Geologic map of California, San Bernardino sheet, California.

Rogers, T.H., 1965. Geologic map of California, Santa Ana sheet, California.

Sankey, J.B., Kreitler, J., Hawbaker, T.J., McVay, J.L., Miller, M.E., Mueller, E.R., Vaillant, N.M., Lowe, S.E., Sankey, T.T., 2017. Climate, wildfire, and erosion ensemble foretells more sediment in western USA watersheds. Geophys. Res. Lett. 44, 8884–8892. https://doi.org/10.1002/2017GL073979

Schwartz, G.E., Alexander, R.B., 1995. Soils data for the conterminous United States derived from the NRCS State Soil Geographic (STATSGO) Data Base: U.S. Geological Survey Open-File Report 95–449. https://water.usgs.gov/GIS/metadata/usgswrd/XML/ussoils.xml (accessed 9.4.20).

Scott, K.M., 1971. Origin and sedimentology of debris flows near Glendora, California, in Geological Survey Research. U.S. Geol. Surv. Prof. Pap. 750-C C242–C247.

Scott, K.M., Williams, R.P., 1935. Erosion and sediment yields in the Transverse Ranges,

southern California. U.S. Geol. Surv. Prof. Pap. 1030 1–38.

Sommerfeld, A., Senf, C., Buma, B., D'Amato, A.W., Després, T., Díaz-Hormazábal, I., Fraver, S., Frelich, L.E., Gutiérrez, Á.G., Hart, S.J., Harvey, B.J., He, H.S., Hlásny, T., Holz, A., Kitzberger, T., Kulakowski, D., Lindenmayer, D., Mori, A.S., Müller, J., Paritsis, J., Perry, G.L.W., Stephens, S.L., Svoboda, M., Turner, M.G., Veblen, T.T., Seidl, R., 2018. Patterns and drivers of recent disturbances across the temperate forest biome. Nat. Commun. 9. https://doi.org/10.1038/s41467-018-06788-9

Staley, D.M., Kean, J.W., Rengers, F.K., 2020. The recurrence interval of post-fire debris-flow generating rainfall in the southwestern United States. Geomorphology 370, 107392. https://doi.org/10.1016/j.geomorph.2020.107392

Staley, D.M., Negri, J.A., Kean, J.W., Laber, J.M., Tillery, A.C., Youberg, A.M., Kimball, S.M., 2016. Updated logistic regression equations for the calculation of post-fire debris-flow likelihood in the western United States. https://doi.org/10.3133/ofr20161106

Tang, H., McGuire, L.A., Rengers, F.K., Kean, J.W., Staley, D.M., Smith, J.B., 2019. Evolution of debris-flow initiation mechanisms and sediment sources during a sequence of postwildfire rainstorms. J. Geophys. Res. Earth Surf. 124, 1572–1595. https://doi.org/10.1029/2018JF004837

Valenzuela, R.A., Kingsmill, D.E., 2015. Orographic precipitation forcing along the coast of northern California during a landfalling winter storm. Mon. Weather Rev. 143, 3570–3590. https://doi.org/10.1175/MWR-D-14-00365.1

Vose, J., Peterson, D., Patel-Weynand, T., 2012. Effects of climatic variability and change on forest ecosystems: A comprehensive science synthesis for the U.S. forest sector.

Wentworth, C.M., Yerkes, R.F., Allen, C.R., 1971. Geologic setting and activity of faults in the

San Fernando area, California. With a section on seismological environment. Geol. Surv. Prof. Pap. 6–16.

Woodhouse, C.A., Meko, D.M., Bigio, E.R., 2020. A long view of southern California water supply: Perfect droughts revisited. JAWRA J. Am. Water Resour. Assoc. 56, 212–229. https://doi.org/10.1111/1752-1688.12822

Wuebbles, D.J., Fahey, D.W., Hibbard, K.A., DeAngelo, B., Doherty, S., Hayhoe, K., Horton, R., Kossin, J.P., Taylor, P.C., Waple, A.M., Yohe, C.P., 2017. Executive summary. Climate science special report: Fourth national climate assessment, volume I. Washington, DC. https://doi.org/10.7930/J0DJ5CTG

Yue, X., Mickley, L.J., Logan, J.A., Kaplan, J.O., 2013. Ensemble projections of wildfire activity and carbonaceous aerosol concentrations over the western United States in the mid-21st century. Atmos. Environ. 77, 767–780. https://doi.org/10.1016/j.atmosenv.2013.06.003